GEOLOGICA CARPATHICA, 2024, 75, 4, 279–299 https://doi.org/10.31577/GeolCarp.2024.16

Miliolid-rich assemblages in the Paratethys: Paleoenvironmental implications for Serravallian (Badenian–Sarmatian) sediments

JAROSLAVA BABEJOVÁ-KMECOVÁ[1,✉], NATÁLIA HUDÁČKOVÁ[1], EDIT KIRÁLY[2], KATALIN BÁLDI[3], NEREO PRETO[4], MÁRIUS BIELICH[1] and MARIÁN GOLEJ[5]

[1]Department of Geology and Paleontology, Faculty of Natural Sciences, Comenius University, Ilkovičova 6, 842 15 Bratislava, Slovakia
[2]Mining and Geological Survey of Hungary, Stefánia út 14, 1143 Budapest, Hungary
[3]Department of Physical and Applied Geology, Faculty of Natural Sciences, Eötvös Loránd University, Pázmány Péter St 1/c, 1117 Budapest, Hungary
[4]Department of Geosciences, University of Padova, Via Giovanni Gradenigo 6, 35131 Padua, Italy
[5]Earth Science Institute, Slovak Academy of Sciences, Dúbravská cesta 9, 840 05 Bratislava, Slovakia

(Manuscript received May 15, 2024; accepted in revised form November 4, 2024; Associate Editor: Matúš Hyžný)

Abstract: The presented multiproxy study sheds light on the intricate interplay between the biological and environmental factors which shaped the middle Miocene landscapes of the Paratethys region. Moreover, they highlight the diverse and dynamic nature of these ancient ecosystems. Here, we study the reasons for the predominance of nine miliolids in the Badenian and Sarmatian sediments, validate systematic and morphogroup approaches using geochemical methods, and finally reveal the bio stratigraphic potential of miliolid horizons during the Serravallian (late Badenian–Sarmatian). Trace elements (Mg/Ca, Ba/Ca, Mn/Ca) from the *MZ 102* borehole and isotopic ($\delta^{18}O$, $\delta^{13}C$) analyses from *ŠVM 1* and *MZ 102* were measured. On the basis of the morphogroup division, an autecological comparison, and geochemical analyses, three main (MG 1, 2, 3) and two small (SG 1, 2) miliolid groups representing distinct microhabitats were characterised. Specific faunal communities (MG 1) document the environment of arborescent algae, such as *Cutleria* and *Fucus* in detritus-rich water substrates, which can lead to suboxia or anoxia in muddy-sandy sediment layers. Other associations (MG 2) correspond to shallow marine environments of hypo/hypersaline lagoons overgrown by short-stemmed arborescent algae, such as *Padina*, *Halopteris*, and *Pseudolithophyllum*, as well as notable salinity fluctuations. Host faunal communities (MG 3) inhabiting the inner shelf are characterized by motile epiphytic foraminifera on algae and *Posidonia* rhizomes. The observable changes to the paleoenvironment can be characterized by fluctuations in salinity and the occasional depletion of oxygen at the bottom.

Keywords: miliolids, Serravallian, Badenian, Sarmatian, Paratethys, geochemistry, stable isotopes, trace elements

Introduction

During the Cenozoic, the geodynamic development of the Eastern Alpine and Western Carpathian highly influenced the paleogeography of Eurasia. The subduction of the European platform during the Eocene/Oligocene boundary led to the final disintegration of the Tethys Ocean (Báldi 1980; Harzhauser et al. 2002; Harzhauser & Piller 2007; Kováč et al. 2017a, b). Along with the developing Mediterranean Sea, the next stage of the disappearing Tethys Ocean was the development of the numerous basins of Eurasian Paratethys (Laskarev 1924) with periodic connections between them (Steininger & Rögl 1984; Nevesskaja et al. 1993; Rögl 1998, 1999; Il'ina 2000; Kováč 2000; Popov et al. 2004; Báldi 2006; Harzhauser & Piller 2007; Piller et al. 2007; Kováč et al. 2017a). During the Neogene, the connection between these two, as well as among the individual basins of Paratethys, became unstable. The periods when the Paratethys was isolated resulted in the formation of endemic fauna and divided it into the extensive Eastern Paratethys "Euxian–Caspian Region" and the smaller parts of the Western (Alpine) and Central (Carpathian, Balkan) Paratethys (Seneš 1961a, b; Popov et al. 2004; Báldi 2006; Piller et al. 2007; Gozhyk et al. 2015; Neubauer et al. 2015; Kováč et al. 2017a, b). The Central Paratethys includes the Pannonian basin system and extends from the foreland of the East Alpine Basin of lower Austria to Moldova (Nevesskaja et al. 1993).

The study of planktic and benthic foraminifera in the sediments of the Central Paratethys has historically been very important for the biostratigraphy (Łuczkowska 1974; Cicha et al. 1998; Andrejeva Grigorovič et al. 2001; Báldi 2006; Kováč et al. 2007; Piller et al. 2007; Abdul Aziz et al. 2008; Holcová 2008; Galović & Young 2012; Hohenegger et al. 2014), paleoceanography (Steininger et al. 1976; Rögl et al. 1978; Rögl & Steininger 1983; Steininger & Rögl 1984; Rögl 1998; Kováč et al. 2007; Piller et al. 2007; Palcu et al. 2015; Kováč et al. 2017a,; Kranner et al. 2021a, b) and interpretation of

✉ corresponding author: Jaroslava Babejová-Kmecová
kmecova45@uniba.sk

the paleoenvironment of marine deposits (Kováč et al. 1997; Kováč & Zlinská 1998; Hudáčková et al. 2009, 2020; Kováčová et al. 2009).

The miliolid foraminifera as taxa are well known for their specific environmental requirements, living conditions, varying limits of salinity tolerance, oxygen content of the surrounding water, and the substrate in which they live (Hallock 1988a, b; Sen Gupta 2003; Murray 2006; Hohenegger 2011). Their calcareous tests are composed of high-magnesium calcite with typical rhomboid structure crystals of different sizes, arranged in three layers (Parker 2017). Recently, DNA extraction (Pawlowski et al. 2013) and wall ultrastructure (Parker 2017) of miliolids were used for identification and determination of species. A comparison of external features of tests is used for taxonomy (Łuczkowska 1964, 1974). Associations of the Miliolida order are particularly prevalent in lagoonal environments, marshes, and the inner shelf, where they live as epifauna, infauna, or epiphytes, often in symbiotic relationships with various types of endosymbionts (Hallock 1988a, b; Sen Gupta 2003; Murray 2006; Hohenegger 2011). However, insufficient attention has been given to small miliolids with the exception of the works by Łuczkowska (1972; 1974).

For the Neogene period (middle Miocene) of the Paratethys, the sediments with a predominance of miliolids were analysed in the Polish Carpathian Foredeep Basin (Łuczkowska 1964, 1974; Dumitriu et al. 2017, 2018, 2020), the Eastern Carpathian Foreland Basin in Romania, and the Republic of Moldova (Moldavian platform; Dumitriu et al. 2017, 2018, 2020), as well as in the Slovak basins, e.g., the Vienna Basin (Čierna 1974; Rohalová & Hash 2000; Koubová & Hudáčková 2010; Zlinská et al. 2010; Hudáčková & Keblovská 2012; Babejová-Kmecová et al. 2022), the Danube Basin (Kováč et al. 2008), and in the East-Slovakian Basin (Hudáčková et al. 2001). For this study, we collected samples and data from several localities with horizons of predominance of miliolids "miliolid horizons" (MH). Miliolids were found exclusively in a hypersaline paleolake situated in the northern part of Central Anatolian Plateau (Turkey; Mazzini et al. 2013; Babejová-Kmecová 2020).

The aim of this work is to study the middle Miocene sediments with a predominance of miliolids from various locations in the Paratethys. Our study attempts: (a) to determine the reason for the predominance of miliolids in these sediments; (b) to compare systematic and/or morphogroup approach results and prove their validity with results of geochemical methods; (c) to reveal the biostratigraphic potential of miliolid horizons, and (d) to interpret the paleoenvironmental conditions during the Serravallian (late Badenian–Sarmatian).

Geological setting

The Vienna Basin (VB), which is located at the junction of the Eastern Alps and the Western Carpathians, is a SW–NE oriented Neogene basin. It is approximately 200 km long and 50 km wide (Kováč et al. 2004), and its depth in the central part reaches over 5500 m (Kilényi & Šefara 1989). It extends over the territory of Austria, the southern part of Czech Republic, and the western part of Slovak Republic. From the Vienna Basin, we collected samples from several localities (Fig. 1): Malacky gas storage cores *MZ 102*, *MZ 93*, and *MZ 34* located near the town of Malacky, Slovakia (Koubová & Hudáčková 2010; Zlinská et al. 2010; Babejová-Kmecová et al. 2022); borehole core *Rohožník 112* from the Rohožník–Konopiská clay pit (Slovakia; Čierna 1974; Rohalová & Hash 2000), *Suchohrad 63*, drilled 4 km SW from the village of Gbely (Hudáčková et al. 2004), and from the cores *Poddvorov 96* and *Poddvorov 118*, located near the village of Poddvorov (Bojanovice) in the south of the Czech Republic.

The Danube Basin (DB) is located south of the Vienna Basin (Fig. 1) and is separated from it by the Malé Karpaty (Small Carpathian Mountains). It represents the northernmost part of the Pannonian Basin System, and it is situated partially in Northwest Hungary and in Eastern Austria as well. From the Danube Basin, we collected samples from borehole *ŠVM 1* located near the village of Tajná, as well as from the eastern part of the Komjatice depression (Kováč et al. 2008) and the borehole *Ivanka 1* (Zahradníková et al. 2013; Šarinová et al. 2018).

The Eastern Slovak Neogene Basin (ESNB; Fig. 1) is an autonomous section of the Transcarpathian Basin. It is almost 90 km long and 40 km wide, ranging from the cities of Košice to Prešov, located in Northeast Slovakia (Kováč et al. 1996; Baráth et al. 1997; Kováč & Zlinská 1998; Vass 2002). The studied samples were collected from the Albinov borehole (core *Albinov 4*) located near the city of Trebišov (Hudáčková et al. 2001).

Data from the Carpathian Foredeep and the Moldavian platform were taken from the published literature by Dumitriu et al. (2017), in which a more detailed description is available (Supplement).

For this study, we also used samples from sediments predominated by miliolids from the Turkish paleolake (the *Tuğlu* section; Cankiri Basin; Fig. 1), which is situated in the northern part of the Central Anatolian Plateau (Turkey; Mazzini et al. 2013; Babejová-Kmecová 2020).

Vienna Basin

Borehole *MZ 102* is situated west of the town of Malacky, and the samples were collected from the Hrušky (Studienka Mb.) and Holíč Formation cores: No. 6 (1051.6–1060.1 m), No. 5 (1043.1–1051.6 m), No. 4 (1034–1043.1 m), No. 3 (652.2–659.8 m), and core No. 2 (644–651 m). Badenian and Sarmatian stages were identified (Fig. 2) with *Bulimina/Bolivina* Zone and the *Porosononion granosum* Zone with associations of *Articulina problema*, *Varidentella rotunda*, *Porosononion granosum*, and *Ammonia* spp. (Fig. 2). These cores' sediments primarily comprise well-sorted sandstones within a matrix of fine-grained claystones ranging in colour from bright to dark grey, occasionally containing coal

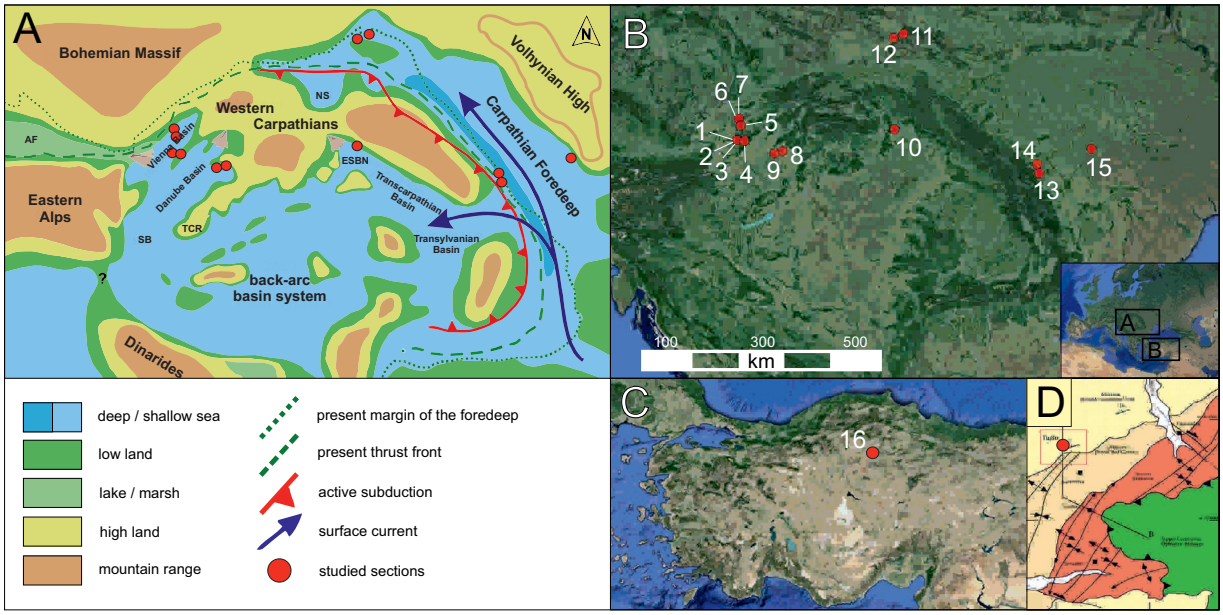

Fig. 1. Localization map: **A** — The Central and part of the Eastern Paratethys during the middle Miocene (Kováč et al. 2017b); **B** — Central Europe today; **C** — Central Anatolia (Mazzini et al. 2013); **D** — Geological map – Çankiri basin; with studied sections and their locations: 1, 2 and 3 – Malacky gas storage (boreholes *MZ 102*, *MZ 93* and *MZ 34*); 4 – *Suchohrad 63*; 5 – *Rohožník 112*; 6, 7 – *Poddvorov 96* and *Poddvorov 118*; 8 – *ŠVM 1*; 9 – *Ivanka 1*; 10 – *Albinov 4*; 11 – *Jamnica M 83*; 12 – *Machów*; 13 – *Dorneşti* outcrop; 14 – *Rădăuţi* core; 15 – *Costeşti* section; 16 – *Tuğlu* outcrop. Paleogeographic reconstructions of the Central Paratethys were taken from Kováč et al. (2017b). Explanatory notes: (AF) Alpine Foredeep, (SB) Styrian Basin, (TCR) Transdanubian High, (NS) Nowy Sącz piggy-back Basin, (ESBN) The East Slovakian Neogene Basin, (?) assumed short living sea connection.

deposits. A comprehensive sedimentological analysis has previously been published (Babejová-Kmecová et al. 2022).

The second borehole *MZ 93* is situated nearby, and the Sarmatian stage (Holíč Formation) was determined (Koubová & Hudáčková 2010). The foraminifera were studied in cores No. 5 (874–870 m), No. 4 (869–861 m), No. 3 (859–857.5 m) and core No. 2 (630.5–623.5 m), which contain the benthic index species *Elphidium hauerinum*, *Anomalinoides dividens*, and associations of Sarmatian biozones, such as *Ammonia*, *Anomalinoides dividens*, *Elphidium reginum*, and *Porosononion granosum.* The cores embodied *Ostracoda* fragments and fish bones. In the lowermost part, the sediments were defined as grey fine clayey sands and grey-brown granulose sands. Core-top sediments consist of clayey sands laminated with fine-grained sands and coal layers (Koubová & Hudáčková 2010).

The sediments examined from borehole *MZ 34*, which concludes core No. 2 (1035–1031 m) and No. 1 (1031–1025 m), were identified as Lower Sarmatian deposits (Holíč Formation) with associations of the genera *Articulina* and *Miliammina*, the species *P. granosum*, and the *Elphidium reginum* Zone. The sediments comprise clays and bioturbated silts with sand intercalations (Zlinská et al. 2010).

The borehole *Suchohrad 63* was drilled at a total depth of 2018 m and the processed length, which was completely cored, comes from the interval of 626.0–681.3 m (Hudáčková et al. 2004). Biostratigraphy was determined as Badenian (Studienka Formation) to Sarmatian (Holíč and Skalica formations) by the presence of foraminifera associations (*Quinqueloculina akneriana*, *Ammonia tepida*, *P. granosum*, *E. hauerinum*), calcareous nannoplankton, ostracods and pollen content. The sediments were predominantly clays, silts, and sands (Hudáčková et al. 2004).

The *Rohožník 112* borehole is located in the Rohožník–Konopiská locality and reaches depths of 30–100 m. When examined, the Sarmatian strata of the Holíč Formation contained the fauna of two zones: a Lower Sarmatian with *Elphidum reginum* Zone (*E. reginum*, *E. hauerinum*, *E. antonium*, *E. fichtelianum*) with various miliolids, mainly *Articulina* spp. (Čierna 1974) with an abundant presence of mollusc assemblages. The sediments contained clays and sand with silts horizons (Švagrovský 1971, 1981; Meszároš 1986; Fuksi 2015).

The samples from the borehole *Poddvorov 96* come from one core No. 1 (1566.9–1558.9 m). Age was determined as Badenian (Hrušky Formation) with the presence of *Ammonia inflata* with keeled elphidiids and large symbiont bearing miliolids, such as *Peneroplis* and *Borelis*. With the exception of foraminifers, the sediments embodied fossil ostracods, fragments of molluscs, echinoderms, spicules, and fish bones. The upper part consists of loose, coarse-grained sand sediments with predominant quartz grains. Towards the base, the sediments become finer with the presence of quartz, pyrite, and plant coal. The *Poddvorov 118* borehole with one core N. 1 studied is equivalent to the *Poddvorov 96* with the same stratigraphic stage; however, foraminiferal associations consist of *Ammonia parkinsoniana*, *A. inflata*, and small

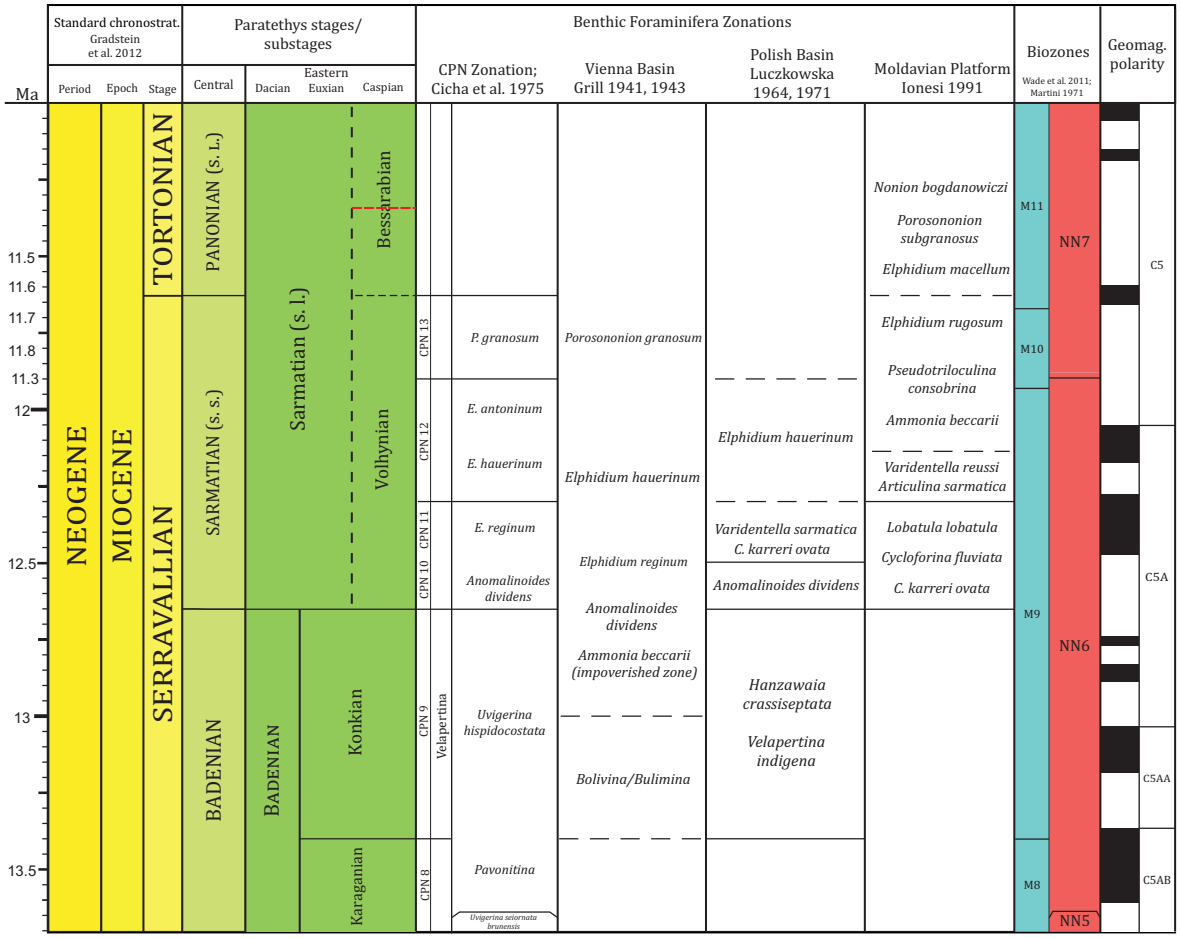

Fig. 2. Correlation chart: Standard chronostratigraphy and Paratethys stages/substages; created using Time Scale Creator (Gradstein et al. 2012; red line modified after Raffi et al. 2020) with benthic foraminifera zonations.

miliolids, *Cycloforina contorta* and *Varidentella latelacunata* and *Haynesina* sp. Study of the sediments revealed that they also contained foraminifera ostracods and bivalves with light grey, coarse-grained sandstones (Hudáčková & Keblovská 2012).

Danube Basin

The borehole *ŠVM* 1 was drilled to a total depth of 211 m. Foraminifera were studied in the interval of 182.5–71.6 m with the Sarmatian/Pannonian age for the Vráble and Ivanka formations. The studied Sarmatian samples embodied foraminifera of the *Elphidium reginum* Zone, a small miliolids zone with ostracods and fish remains (Kováč et al. 2008). The sedimentary record consists of green to greenish-brown claystones, while towards the base, brownish-green laminated claystones are present (Kováč et al. 2008).

The samples from the borehole *Ivanka 1* (total depth 2390 m, 34 cores) were collected from cores with predominance of miliolids: core No. 15 (2093–2090 m), No. 14 (2045–2040 m) and No. 12 (1061–1056 m), all belonging to the Sarmatian stage (Vráble Formation) and supported by the presence of *E. hauerinum* and *Bolivina sarmatica* (Šarinová et al. 2018). Apart from miliolids (dominated by *Miliolinella subrotunda)*, *Ammonia tepida*, *A. parkinsoniana*, *Elphidium* spp., *Nonion* spp., *Bolivina* spp., and *P. granosum* are present. The sediments are dominated by mudstones and sandstones with fish remains, coal, and organic matter (Zahradníková et al. 2013; Šarinová et al. 2018).

East Slovakian Basin

The borehole *Albinov 4* samples were collected from the cores in intervals of 650–453 m (core No. 6, 5 and 4) and of 105–100 m (core No. 2) with sediments determined as upper Badenian to Sarmatian from the Klčovo and Stretava formations (Hudáčková et al. 2001). The foraminiferal associations are composed of small miliolids (*Quinqueloculina buchiana*, *Quinqueloculina hauerina*, *Quinqueloculina bogdanowiczi*, *Quinqueloculina akneriana*) accompanied by *Elphidiella artiflex*, *Elphidium joukovi*, *Elphidium macellum*, and *Ammonia viennensis*. Lithology is predominantly calcareous sandstones and mudstones, with volcanic glass fibres known as Pelea's hair (Hudáčková et al. 2001).

Polish Carpathian Foredeep Basin

Boreholes *Jamnica M83* and *Machów* (depth 0–75 m) chronostratigraphically range from upper Badenian to Sarmatian stages (Machów Formation). Foraminiferal assemblages are represented by species *Globigerina bulloides, Uvigerina semiornata, Anomalinoides dividens, and numerous* miliolid foraminiferal associations: *Jamnica M83* consists of abundant occurrence of *Articularia articulinoides*, *Pseudotriloculina consobrina*, and *Triloculina inflata*; in the Machów formation: *Spirosigmoilina tenuis*, *Varidentella reussi, Q. akneriana* (Dumitriu et al. 2017). The sediments are characterized by clays and mudstones.

Eastern Carpathian Foredeep Basin

The sediments of the *Rădăuţi* core section (depth 250 m), the *Dorneşti* outcrop (depth from 380–355 m) of the Lespezi Formation, and the *Costeşti* section (132–115 m) of the Darabani–Mitoc Clays and Stanca Limestone Formations, were all identified as lower Sarmatian (Dumitriu et al. 2017). In the *Rădăuţi* core section, numerous foraminiferal species were identified, dominated by elphidia, ammonia, and various species of miliolids: *Cycloforina cristata*, *Cycloforina predcarpatica*, *Cycloforina karreri ovata, Cycloforina karreri karreri, C. predcarpatica* and *C. fluviata, Varidentella pseudocostata, V. rotunda*, and *Q. akneriana* (Dumitriu et al. 2017). The samples from the *Dorneşti* outcrop contained the species *Lobatula lobatula* and *L. elphidia*, as well as the miliolids *Articularia karreriella*, *C. karreri ovata*, *C. karreri karreri*, and *C. predcarpatica.* The *Costeşti* section samples yielded foraminiferal associations of small miliolids, such as *P. consobrina*, *P. consobrina nitens*, *A. problema*, *A. articulinoides* etc., and hyaline forms, such as *Porosononion subgranosus*, *P. martkobi*, and *Fissurina cubanica*. Sediments are represented by clays with fine intercalations of sand, sandstones, and coal (Dumitriu et al. 2017).

The samples that come from Central Anatolia (*Tuğlu* section, depth 0–10 m) were determined as Sarmatian, Tuğlu Formation (Mazzini et al. 2013). Identified foraminifera associations were abundant, but with low species diversity, consisting only of miliolids, such as *Q. akneriana*, *Miliolinella banatiana*, *M. subrotunda*, and *M. suborbicularis* (Babejová-Kmecová 2020). Fossil records included nannoplankton, ostracods, molluscs, and small mammal assemblages. Sediments are predominantly composed of dark grey silts located in between two layers of sandstones with rich organic compound (Mazzini et al. 2013).

Material and methods

Laboratory work

Laboratory work involved drying the separated samples (100 g of each sample), dilution by 5 % hydrogen peroxide, and wet screening of the rock material with wire screens between 0.071–1 mm and more. When possible, 250 individuals of benthic foraminifera were picked out of the residua. Foraminifera were separated under the stereo microscope ZEISS Stemi 508 and then observed and documented (Fig. 3) using the electron scanning microscope QUANTA FEG 250. Collected individuals were determined into taxonomic categories according to Cicha et al. (1998), Łuczkowska (1972, 1974), and Maisuradze (1971), which are explicitly focused on miliolid rich sediments. The sedimentary material from the Slovak localities is stored at the Department of Geology and Palaeontology at Comenius University in Bratislava.

Statistical methods

Statistical analyses were used to identify and evaluate factors that influence the diversity and distribution of foraminifera in time and space (species-diversity of benthic foraminifera evaluated by the Fisher alpha and Shannon_H indices, principal component analysis (PCA), the Ammonia–Elphidium index, Taxa_S, Dominance_D, element/Ca measurements, and $\delta^{18}O$ and $\delta^{13}C$ analyses; Figs. 4–9). The calculations for this study specifically targeted samples containing miliolid species (MH) and comprising 15 % or more of the total composition. Statistical data were analysed using the statistical program R (R Development Core Team 2016), PAST – Paleontological Statistics version 4.10 (Hammer et al. 2001) and Microsoft Excel (Microsoft Corporation 2018). Foraminifera shells were divided into the morphogroups EP-A+B, EP-C and EP-D (Langer 1993) and according to their ecological preferences (Murray 2006; Supplement). Information regarding the ecological requirements of miliolid foraminifera (Table 1) was derived from the studies of Łuczkowska (1972, 1974); Steineck & Bergstein (1979); Hallock (1988a, b); Kaiho (1991, 1999); Langer (1993); Murray (1991, 2006); Hohenegger (2011); Dubicka et al. (2015); Dumitriu et al. (2017, 2018).

LA-ICP-MS method

The composition of trace elements in foraminifera calcite (Mg/Ca, Ba/Ca, Mn/Ca) was measured in the most abundant miliolid species: *A. problema*, *V. rotunda*, *P. consobrina*, *M. subrotunda*, *Siphonaperta lucida*, and one hyaline species, *P. granosum*, from the *MZ102* borehole. Mg/Ca composition was calculated in $mol.mol^{-1}$, Ba/Ca, and Mn/Ca ratios; composition was calculated in $mmol.mol^{-1}$. Ratios were determined by LA-ICP-MS at the Mining and Geological Survey of Hungary, Budapest. The analyses were performed using a New Wave UP213 Nd:YAG laser ablation system attached to a Perkin Elmer Elan DRCII type quadrupole ICP-MS. The ablated aerosol was delivered to the mass spectrometer by He gas (0.9 l/min mixed with Ar gas (0.8 l/min). Frequency, spot size, and laser energy were carefully chosen to get the longest and the largest signal from the foraminifera, 5 Hz, 80 µm, and 7.2–7.6 J/cm^2 respectively. The analyses of ^{7}Li,

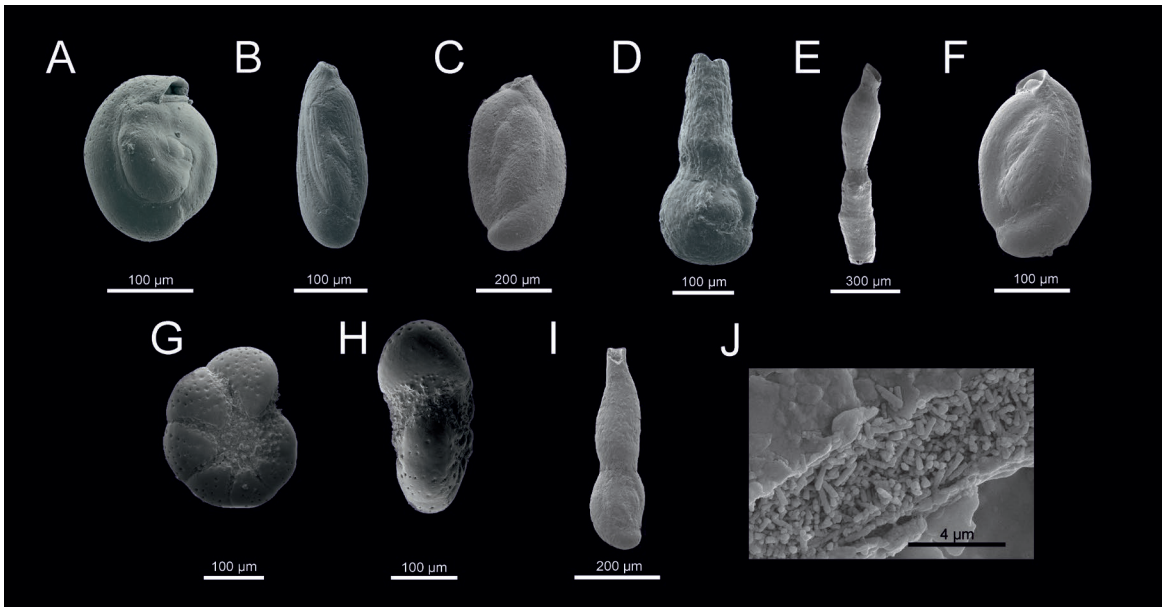

Fig. 3. SEM photographs of foraminifera species found in *MZ 102*. **A** — *Miliolinella subrotunda* (depth 647.8 m); **B** — *Pseudotriloculina consobrina* (depth 654.5 m); **C** — *Quinqueloculina seminulum* (depth 648.35 m), **D, E** — *Articulina problema* (depth 648 m); **F** — *Varidentella rotunda* (depth 647.8 m); **G, H** — *Porosononion granosum* (depth 649.2 m); **I** — *Articularia articulinoides* (depth 647.8 m); **J** — wall detail of *A. problema* (depth 648 m).

^{23}Na, ^{25}Mg, ^{26}Mg, ^{29}Si, ^{43}Ca, ^{55}Mn, ^{63}Cu, ^{64}Zn, ^{65}Cu, ^{66}Zn, ^{88}Sr, ^{135}Ba, ^{137}Ba, and ^{138}Ba (with 10 ms dwell time) were measured. We tested the reference materials of MACS3, NIST612, and 610. NIST610 was proven to be the most stable as an external standard, while 40 % of CaO was chosen for internal standard. BCR-2G was periodically analysed as unknown in order to check for the quality of analyses. The external standards MACS3 and NIST610 and control material BCR-2G were measured after every 8–19 spots. The evaluation of data was done by the software Sills (ETH Zürich) and the results are in mol/mol and µmol/mol ratios with reference to Ca. REE concentrations were normalized to 40 % of CaO. While resolving the method for LA-ICP-MS analyses, we tried single shells on blue tech, buried in epoxy and glued on the glass. The shells in epoxy worked extremely well, especially the signal, which was long enough to evaluate. The blue tech and glass contaminated the signals derived from the foraminiferal shells. All of the LA-ICP-MS measurements were averaged (Species/Samples) and added to the graphs. The AES-ICP measurements were all performed from the entire bulk of samples, and the values were also added to the graph.

Stable isotopes

For purposes of geochemical isotope δ^{18}O and δ^{13}C analyses, the sedimentary material from *ŠVM1*/173–173.2 m and *MZ102*/646.1–649.2 m was selected and carefully sampled. We selected approximately ten individuals from each sample of *ŠVM1* (*Bolivina variabilis, A. viennensis*) and around fifty individuals from *MZ102* (*A. problema*, *P. granosum*, *V. rotunda*, *P. consobrina*, *M. subrotunda*, *S. lucida*) due to the presence of smaller individuals. These individuals were observed under the SEM (scanning electron microscope Hitashi Quanta FEG 250, SAS SR) for its preservation state. The state of preservation was evaluated for each individual foraminifera test, based on the character of the inner wall structure. Analyses of stable isotopes of carbon and oxygen were performed on multiple individuals from each species in order to capture the variability of isotopic values. Isotope analyses were carried out at the Earth Science Institute of the Slovak Academy of Sciences laboratories in Banská Bystrica (Slovakia) and at the Department of Geosciences, University of Padua (Padua, Italy). Analyses were performed on a MAT 253 and Delta V Advantage gas isotope ratio mass spectrometers (Thermo Scientific) coupled with a Kiel IV (Thermo Scientific) automatic preparation line, where the carbonates were digested in H_3PO_4 at 70 °C in a vacuum following the method of McCrea (1950). CO_2 discharge was cryogenically purified and introduced to a dual inlet system of the mass spectrometer for further isotope measurements. Internal standard deviations in samples from *ŠVM1* for δ^{13}C are 0.018 ‰ min. and 0.193 ‰ max.; for δ^{18}O, it is 0.02 ‰ min. and 0.24 ‰ max. For samples from *MZ102*, internal standard deviations were: for δ^{13}C are 0.01 ‰ min. and 0.10 ‰ max.; for δ^{18}O, it is 0.03 ‰ min. and 0.10 ‰ max. International reference material NBS18 was used to verify the accuracy of outcome delta values with all values relative to VPDB. Reported isotope values are stated as δ^{13}C and δ^{18}O vs. VPDB. For our study, we used an equation based on the oxygen isotope paleothermometry studies of Urey (1947) and Epstein et al. (1953). Urey (1947) predicted that

Table 1: Ecological requirements of miliolid foraminifera present in our study, derived from Łuczkowska (1972, 1974), Steineck & Bergstein (1979), Hallock (1988a, b), Kaiho (1991, 1999), Langer (1993), Murray (1991, 2006), Hohenegger (2011), Dubicka et al. (2015), Dumitriu et al. (2017, 2018).

Genus	Mode of life	Substrate	T (°C)	Salinity (‰)	Depth/ Environment	Bottom O2
Affinetrina	epifaunal, epiphyte (*Posidonia*)	–	cold/warm	hypersaline	inner shelf	–
Articularia	epifaunal	–	–	–	–	–
Articulina	epifaunal, facultative free	Phytal, muddy sediment	>20	marine – hypersaline	inner shelf, bathyal	–
Borelis	epifauna, facultative free	algal–coated substrates, hard sediment	18–26	normal marine	5–65 m; lagoon – reef	–
Cycloforina	epifaunal	–	warm	marine – hypersaline	inner shelf	–
Miliammina	infaunal – epifaunal, free	mud, silt	0–30	0–50	brakish – hypersaline marshes – upper bathyal	–
Miliolina	epifaunal	sand	warm tropical	brakish – normal marine	high-energy environment	oxic
Miliolinella	epifaunal, free, epiphyte (*Posidonia*, *Sargassum*, *Padina pavonia*)	plants and hard substrates	10–30	32–50	0–100 m, hypersaline lagoons and marshes, inner shelf	–
Peneroplis/ Dendritina	epifaunal, epiphytes (*Dasycladus*, *Halopteris*, *Pseudolitophyllum*, *Posidonia*)	plants and hard substrates	18–27	35–53	lagoons, inner shelf	–
Pseudotriloculina	epifauna, free, epiphytes (*Posidonia*)	mud, sand, plants	warm	marine – hypersaline	inner shelf	–
Quinqueloculina	epifauna, free, epiphytes (*Posidonia*, *Ectocarpus*)	plants or sediment	cold–warm	32–65, marine – hypersaline	hypersaline lagoons, marine shelf, rarely bathyal	oxic/suboxic
Sigmoilinita	epifauna	–	–		mid shelf – bathyal	oxic
Spiroloculina	epifaunal, free, epiphyte	sediment or plants	warm	marine – hypersaline	0–40 m, lagoons, inner shelf	–
Triloculina	epifaunal, free, epiphyte	mud, sand, plants	cold–warm	32–55? marine – hypersaline	mainly hypersaline lagoons or marine inner shelf, some bathyal species (cold)	oxic
Varidentella	epifaunal	–	–	–	shelf	–

the oxygen isotope ratio varies as a function of temperature. The equation used in this study was adapted from the modified version of Shackleton (1974) and Kováčová & Hudáčková (2009) for the calculation of bottom and surface water temperature:

$$T = 16.9 - 4.38\,(\delta^{18}O_c - \delta^{18}O_w) + 0.10\,(\delta^{18}O_c - \delta^{18}O_w)^2$$

where T is the paleotemperature (°C), $\delta^{18}O_c$ is $\delta^{18}O$ of the carbonate incorporated in tests, and $\delta^{18}O_w$ is the isotopic composition of seawater, in which the tests were precipitated in. The value of $\delta^{18}O_w$ is used based on the study of Harzhauser & Piller (2007).

Results

Taxonomy & morphogroups

Species diversity

The Fisher alpha and Shannon_H indices ratio evaluation showed species diversity in all localities (>15 % miliolids). The samples fell into three main groups and one overlapping group, while 11 samples fell outside of these fields (Fig. 4). The first group (A) represents the values of the Shannon_H indices from 0.87 to 2.39 and from 1.39 to 5 of the Fisher alpha index. The group contains samples predominantly from *Poddvorov 96* (P96/5, P96/10, P96/1, P96/12, P96/14, P96/16, P96/2, P96/4, P96/7, P96/9), *MZ102* (MZ102/10, MZ102/2, MZ102/23, MZ102/28, MZ102/3, MZ102/4, MZ102/8, MZ102/9), *Machów* (M/13, M/15, M/16, M/17, M/20, M/25, M/29), and *Jamnica M83* (J/12, J/13, J/2, J/6, J/7, J/8). A second group (B) included values of the Shannon_H indices from 0.3 to 2.47 and from 0.32 to 5.69 of the Fisher alpha index. This group consists of samples predominantly from *MZ102* (MZ102/1, MZ102/11, MZ102/24, MZ102/25, MZ102/27, MZ102/6, MZ102/7), *Tuğlu* (TU/1, TU/2, TU/3, TU/5, TU/7, TU/8), *Costeşti* (C/10, C/12, C/14, C/17, C/19) *ŠVM1* (S/1, S/2, S/3, S/4), and *MZ34* (MZ34/1, MZ34/2, MZ34/8, MZ34/9). The third group (C), with values of the Shannon_H indices from 2 to 2.91 and the Fisher alpha index from 5.38 to 8.27, consists of samples predominantly from the *Machów* location (M/18, M/27, M/31) and *Jamnica 83* (J/9, J/11, J/14).

Principal component analysis

The principal component analysis plot illustrates the correlation between the foraminifera morphogroups (Supplement) grouped according to their dependence on variables

expressing ecological factors (Fig. 5). The first two axes (PC 1 and PC 2) explain 75.65 % variation of the data, which distinguish three major groups (MG 1, 2, 3) and two minor ones (SG 1, 2) that fall into different ordination space. The first major group contains mainly samples from *Poddvorov 96* (P96/10, P96/11, P96/16, P96/5, P96/7, P96/8, P96/9), *MZ 102* (MZ102/10, MZ102/24, MZ102/26, MZ102/27, MZ102/28), and *Suchohrad 63* (SH/1, SH/6) on the X axis reaching negative values from −2.47 to −1.3 and on the Y axis from −0.72 to a positive value of 0.16. The second major group contains samples predominantly from *Poddvorov 96* (P96/1, P96/12, P96/13, P96/14, P96/2, P96/3, P96/4), *Rădăuţi* (R/23, R/4, R/6), *Rohožník 112* (RV/7, RV/9), and *Machów* (M/18, M/19, M/20, M/23) with X negative values from −0.97 to positive 0.26 and on the Y axis from −0.59 to positive 0.18. The third major group composes of samples generally from the following localities: *Tuğlu* (TU/1, TU/2, TU/3, TU/4, TU/5, TU/7, TU/8), *MZ 102* (MZ102/1, MZ102/2, MZ102/25, MZ102/3,

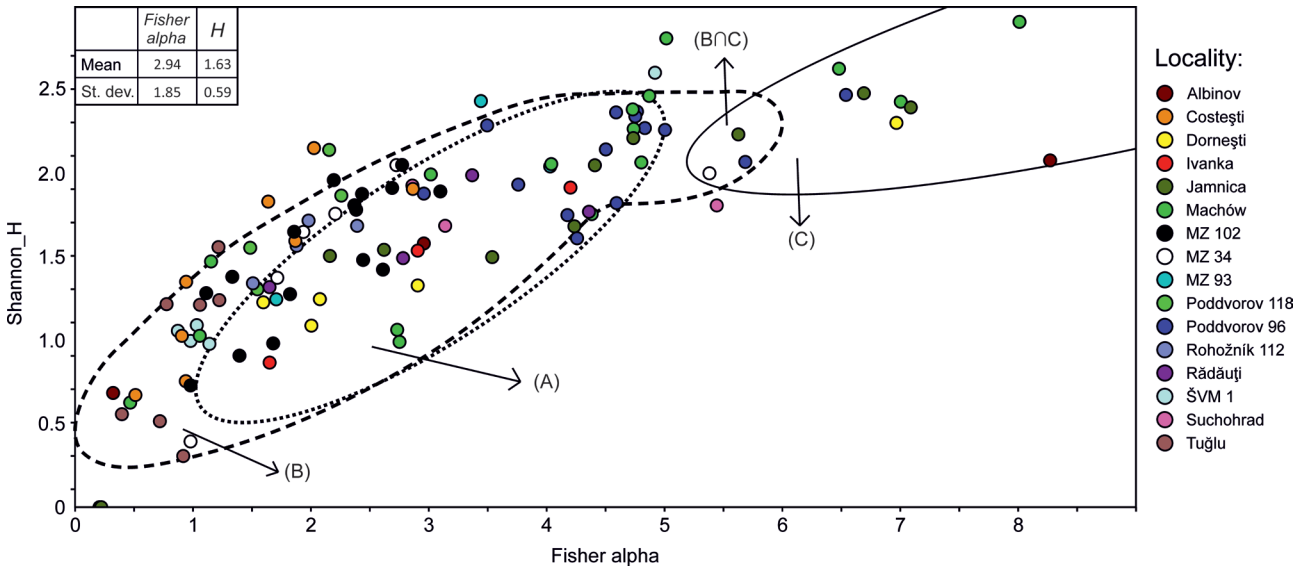

Fig. 4. Diversity plot: Fisher alpha and Shannon_H indices. Samples divided into four environmental groups (A–C) according to their preferences (derived from Murray 2006).

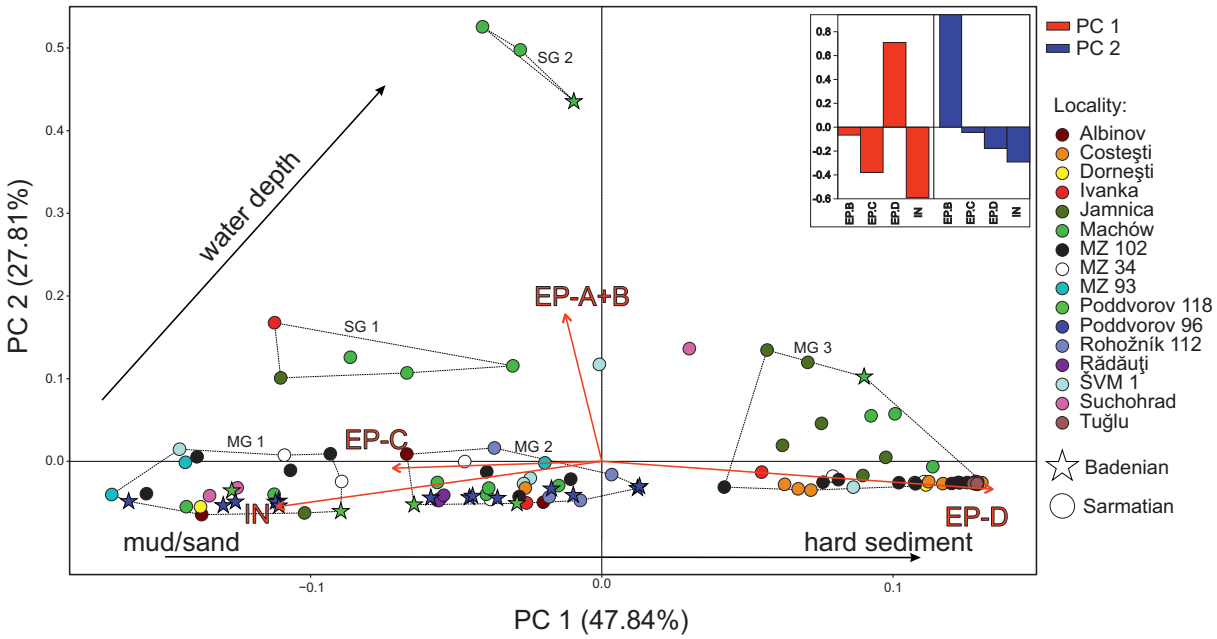

Fig. 5. Principal component analysis plot illustrating the correlation between the foraminifera morphogroups grouped according to their dependence on variables expressing ecological factors. Explanatory notes: MG 1, 2, 3 – major groups 1, 2 and 3; SG 1, 2 – small groups 1 and 2.

MZ102/4, MZ102/6, MZ102/7, MZ102/8, MZ102/9), *Jamnica M83* (J/11, J/12, J/13, J/14, J/2, J/4, J/7, J/9), and *Costeşti* (C/10, C/11, C/12, C/13, C/14, C/17, C/19) with values on the X axis reaching from 0.45 to 1.89 and on the Y axis from −0.39 to 1.52. The small group in the range of values on the X axis from −1.6 to −0.4 and the Y axis from 1.1 to 1.9 is represented by samples from *Machów* (M/24, M/25, M/31), *Ivanka 1* (IV/3), and *Jamnica M83* (J/8). The second small group is interpreted with the samples from *Machów* (M/4, M/8, M/13), with X values from −0.6 to −0.1 and Y values from 4.9 to 5.9. The samples with different biostratigraphic ranking were evaluated – none of the groups showed biostratigraphic relevance (Figs. 5, 6).

Dominance & MH "Miliolid horizons"

The MHs were found in four Badenian levels (*Poddvorov 96, 118* in three depth intervals), while in *Machów*, in one horizon (73 m; Table 2). These horizons contain large miliolid foraminifera, such as *Borelis*, *Peneroplis*, *Q. akneriana*, and *Triloculina gibba* (Table 2; Supplement). In the Sarmatian sediments, 31 MHs were identified (Supplement) with the presence of small miliolids: *Pseudotriloculina, Quinqueloculina*, *Miliammina*, *Articulina*, and *Articularia* (Table 2; Supplement). MH found in *MZ102*: the cores n. 4 and 2 in depth intervals of 1035.5–1034.6 m and 649.2–646.2 m the most abundant species being: *A. problema*, *V. rotunda*, *P. consobrina*, *S. lucida*, *A. articulinoides*, *M. subrotunda*, and *Quinqueloculina seminulum*; as well as the hyaline genera: *Porosononion* and *Cribroelphidium* (Fig. 3). The complete list of MH species and depth intervals from our study can be found in Table 2 (and the Supplement).

Ecological group dominance from MZ102 and ŠVM1

The evaluated results (Fig. 7a, b) show change in salinity and oxic/dysoxic conditions in two stages. The first stage is visible in the depth ranges from 1059.8 to 1041.6 m and from 659.4 to 648.3 m in *MZ102*, and in *ŠVM1* in 182.6 to 173 and 120.5 m, with dominance of brackish/marine, marine, and

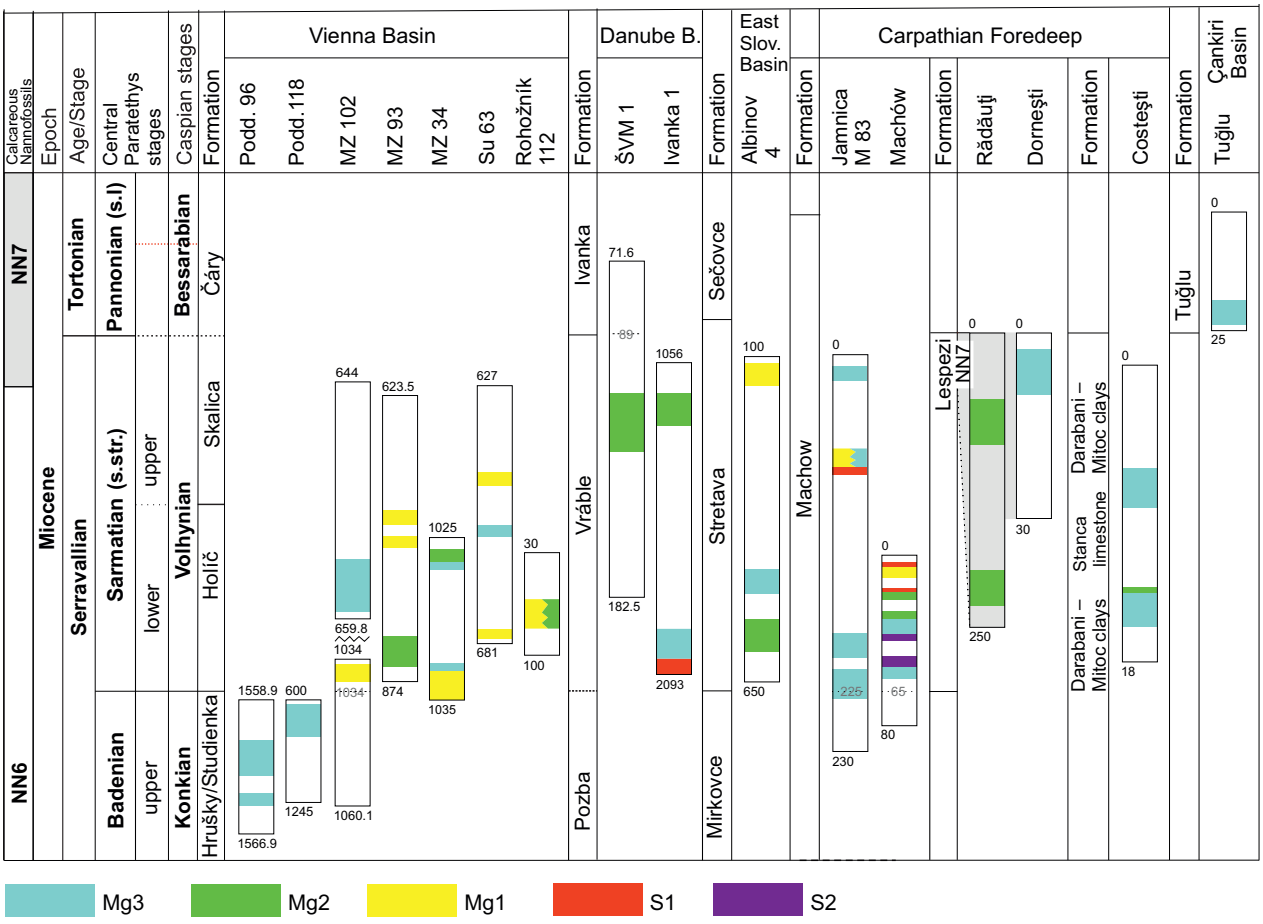

Fig. 6. The figure illustrates the position of MH within the studied wells, indicating their stratigraphic levels and the formations in which they are identified. The correlation of borehole logs represents the best possible approximation. The upper and lower depths of the boreholes and outcrops are shown in metres, along with a potential boundary between geological periods. The thickness of each rectangle reflects the relative thickness of the formation, while the colours, as per the legend, indicate the ecological group of the association (refer to Fig. 5) created using the Time Scale Creator (Gradstein et al. 2012; red line modified after Raffi et al. 2020).

Table 2: List of MH, species, and depth intervals from our study. Explanatory notes: (B) Badenian, (S) Sarmatian.

Locality	Depth intervals (m)	Biostratigraphy	Miliolid species	Other taxa
Vienna Basin				
MZ 102	1035.5–1034.6 649.20–646.20	S	*Articulina problema, Varidentella rotunda, Pseudotriloculina consobrina, Siphonaperta lucida, Articularia articulinoides, Miliolinella subrotunda, Quinqueloculina seminulum*	*Porosononion* sp., *Cribroelphidium* sp.
MZ 93	858.80–858.75 624.57–624.55 624.50–624.40	S	*Affinetrina voloshinovae, P. consobrina, Miliolinella circularis*	*Porosononion granosum, Ammonia viennensis*
MZ 34	~1035–1031 ~1028–1025	S	*Miliammina* sp., *M. circularis, V. rotunda*	*Porosononion* gr. *granosum, Cribroelphidium excavatum*
Suchohrad 63	680.60–680.55 661.56–661.52 637.70–637.50	S	*Quinqueloculina* sp.	*Porosononion* gr. *granosum*
Rohožník 112	~75–50 m	S	*Varidentella reussi, P. consobrina, A. problema*	*E. hauerinum*
Poddvorov 96	1566.40–1566.30 1565.80–1562.75 1560.65–1558.65	B	*Borelis melo, Borelis* sp., *Triloculina gibba, Quinqueloculina aglutinans, Cycloforina badenensis, C. contorta, Peneroplis* sp. , broken miliolid shells	*Ammonia inflata, Elphidium rugosum, Ammonia parkinsoniana*
Poddvorov 118			*C. contorta, Varidentella latelacunata*	*A. parkinsoniana, Haynesina* sp., *Ammonia inflata, Ammonia tepida*
Danube Basin				
ŠVM 1	159.50–114.10	S	*V. rotunda, Quinqueloculina akneriana, A. articulinoides, Articulina sarmatica*	*P. granosum, Ammonia* indet., *Bolivina variabilis, Saccammina* sp., *Elphidium glabrum, Elphidium macellum*
Ivanka 1	2093–2090 1060	S	*M. subrotunda*	*E. macellum*
East Slovakian Neogene Basin				
Albinov 4	656.30–656 553.2–553 446.6–446.3 ~105	S	*Adelosina* ex gr. *schreibersiana, Valvulineria akneriana, V. reussi, V. rotunda*	*A. viennensis*
Polish Carpathian Foredeep Basin				
Jamnica M 83	220–214 202–182 180–173 ~55	S	*P. consobrina, Triloculina pseudoinflata, Affinetrina ukrainica, Q. akneriana, Cycloforina karreri ovata, Cycloforina karreri karreri, Quinqueloculina minakovae ukrainica, A. karreriella, A. articulinoides, V. reussi, V. rotunda, Q. akneriana, M. subrotunda, Miliolinella selene*	*Bolivina moldavica, B. sarmatica, Anomalinoides dividens, E. hauerinum, E. macellum, Elphidiella serena*
Machów	73 57–43 37–30 10	B, S	*Sigmoilinita tenuis, Q. akneriana, V. reussi, P. consobrina, V. rotunda, A. articulinoides, Cycloforina fluviata, C. karreri ovata*	*A. dividens, E. hauerinum, Elphidiella serena, E. macellum, Bolivina moldavica*
Eastern Carpathian Foreland Basin				
Rădăuţi	200–180 77– 46	S	*C. cristata, Q. akneriana, V. rotunda, C. karreri ovata*	*Ammonia beccarii, E. reginum, L. lobatula, Elphidiella serena, E. macellum*
Dorneşti	380–374	S	*C. karreri ovata, Articularia karreriella, Cycloforina predcarpatica, C. karreri karreri*	*Elphidium subumbilicatum, Elphidiella serena*
Costeşti	125–120 118–115	S	*P. consobrina, A. articulinoides, Articulina* sp., *P. consobrina nitens, A. problema, Quinqueloculina* sp.	*P. subgranosus, P. martkobi, Fissurina cubanica, F. isa, F. mironovi*
Central Anatolia				
Tuglu	whole section	S	*Q. akneriana, Miliolinella banatiana, M. subrotunda, M. suborbicularis, Q. guriana, Trisegmentina* sp., *Spiroloculina* sp., *V. reussi*	–

marine/hypersaline with species that prefer living in oxic/suboxic, suboxic, and dysoxic conditions. The second stage is visible in the depth ranges from 1035.8 to 1034.6 m and also from 648 to 641.2 m in *MZ 102*, and in 168 to 142.1 m in *ŠVM 1* with predominance of marine/hypersaline to hypersaline preferred by foraminiferal species that live in oxic, oxic/suboxic to suboxic conditions, mainly miliolids. The IAE index value ranges from 0–100 in the interval 648.3–646.1 m and also with the highest values (100) in 1048.8–1041.6 m; 656.9–652.4 m and 655 m in *MZ 102* and in *ŠVM 1* in 178.3–173.2 m.

Geochemical results

The composition of Mn/Ca had a minimum value of 2.87 mmol.mol^{-1} in the depth of 647.8 m of *P. consobrina* (Fig. 7a, b, c). The highest value of Mn/Ca was found in *S. lucida* at 648.3 metres deep with 61.66 mmol.mol^{-1}. The composition of Mg/Ca in the samples of *MZ 102* ranged from a minimum of 0.19 mol.mol^{-1} in the depth of 648.3 m in *P. granosum* to a maximum of 10.91 mol.mol^{-1} in *A. problema* in the depth of 646.2 m. Ba/Ca ranges from 0.19 mmol.mol^{-1} in *P. granosum* in the depth of 648.3 m, to the highest value of 2.42 mmol.mol^{-1} found in the *A. problema*.

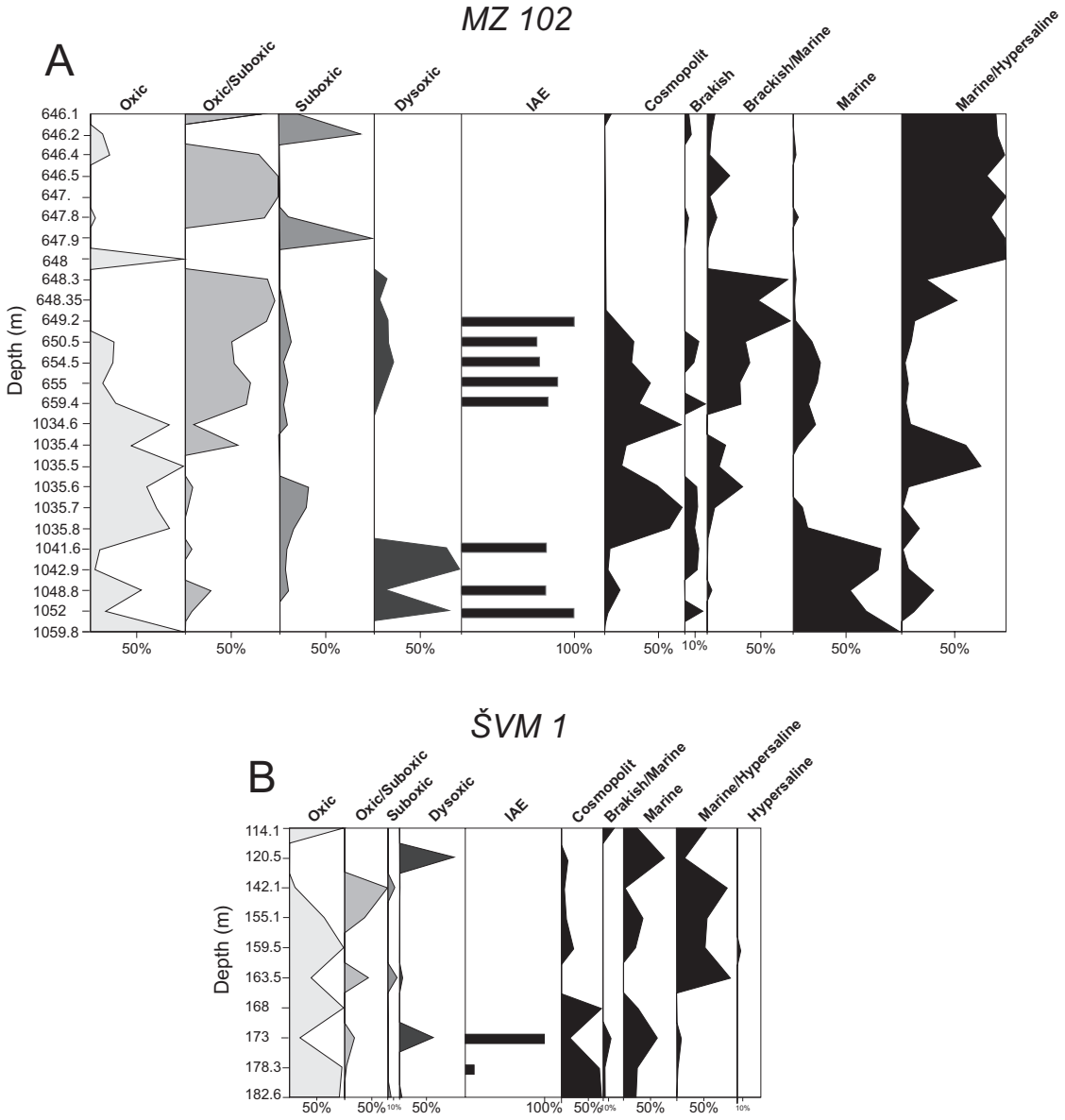

Fig. 7. Stacked area charts showing changes in oxic/dysoxic with the IAE index and salinity conditions in *MZ102* (**A**) and *ŠVM1* (**B**).

Isotopic compositions in *MZ102* of miliolid species for *A. problema* of $\delta^{13}C$ varies from 0.97 to 1.30 ‰ and $\delta^{18}O$ varies from 1.51 to 2.86 ‰ (Table 3). *V. rotunda* $\delta^{13}C$ composition reached values from 1.15 to 1.28 ‰, while $\delta^{18}O$ reached values from 0.38 to 0.79 ‰. For *M. subrotunda* and *S. lucida*, $\delta^{13}C$ reached 1.28 ‰ and 0.67 ‰, and $\delta^{18}O$ values reached 3.12 ‰ and 1.52 ‰. For the last miliolid species *P. consobrina*, $\delta^{13}C$ varies from −0.36 to 2.94 ‰, and $\delta^{18}O$ from 0.43 to 2.56 ‰. The hyaline species of *P. granosum* located at the base of the analysed MH reached $\delta^{13}C$ from −2.60 to −2.28 ‰, and $\delta^{18}O$ from −0.52 to −0.39 ‰. For *ŠVM1*, *B. variabilis*, the isotopic result of $\delta^{13}C$ varies from −1.23 to 0.41 ‰, while $\delta^{18}O$ varies from −0.10 to 3.06 ‰. For *A. viennensis*, the value of $\delta^{13}C$ varies from −1.44 to 1.20 ‰, and the value of $\delta^{18}O$ varies from −2.55 to −1.25 ‰. Comparison of oxygen isotope and carbon isotope variations of foraminifera from *MZ102* and *ŠVM1* are shown in (Fig. 8). Averaged Mg/Ca compositions of all foraminifera shells (miliolids and hyaline) were correlated with the $\delta^{18}O$ values from *MZ102* (Fig. 9). Temperature results vary from 13.36 to 30.03 °C in *MZ102* and from 5.57 to 30.26 °C in *ŠVM1* (Table 3).

Discussion

Biostratigraphy was established based on the studies (Čierna 1974; Rohalová & Hash 2000; Hudáčková et al. 2001, 2004; Kováč et al. 2008; Koubová & Hudáčková 2010; Zlinská et al. 2010; Mazzini et al. 2013; Zahradníková et al. 2013; Dumitriu et al. 2017; Šarinová et al. 2018; Babejová-Kmecová 2020;

Table 3: List of species from *MZ102* and *ŠVM1* and their values of stable isotope analyses ($\delta^{18}O$, $\delta^{13}C$) with temperature in °C calculated according to Shackleton (1974) and Kováčová & Hudáčková (2009).

Core	Sample (m)	Species	$\delta^{18}O$ (‰, V-PDB)	$\delta^{13}C$ (‰, V-PDB)	Temperature (°C)
MZ102	646.1	*A. problema*	1.59	1.13	22.73
		V. rotunda	0.38	1.28	17.25
	646.2	*A. problema*	1.51	1.30	22.34
		V. rotunda	0.79	1.15	19.07
	647.8	*M. subrotunda*	3.12	1.28	30.03
		P. consobrina	2.56	2.94	27.31
	647.9	*A. problema*	2.86	0.97	29.77
	648.3	*S. lucida*	1.52	0.67	22.39
		P. granosum	−0.39	−2.28	13.91
	649.2	*P. granosum*	−0.52	−2.60	13.36
		P. consobrina	0.43	−0.36	17.47
ŠVM1	173–173.2	*B. variabilis*	0.84	−0.52	14.56
		B. variabilis	−0.01	−1.02	18.27
		B. variabilis	−0.10	−1.23	18.67
		B. variabilis	3.06	0.41	5.57
		A. viennensis	−2.55	−1.44	30.26
		A. viennensis	−1.25	1.20	23.95

Babejová-Kmecová et al. 2022). However, the calcareous zonation depicted in Figure 2 presents a generalized zonation for regional stages by Raffi et al. (2020). Notably, their suggested zonation of NN6 and NN7 zones deviates from those mentioned in Dumitriu et al. (2017). Peryt et al. (2024) highlight the ambivalence surrounding the calcareous zonation in the Polish Carpathian Foredeep (*Jamnica M83, Machów*). The delineation of boundaries between NN6 and NN7 is marked with a degree of ambiguity, thus suggesting a broader time span.

Foraminifera and morphogroup approach

According to the results from using the relationship of the Fisher alpha and Shannon_H indices (Figs. 4, 6), the samples that fell into the first group (A) contain assemblages that tolerate a normal marine estuary and lagoonal to hypersaline lagoonal environments. The dependence of this relation of diversity and environment was empirically shown by Murray (2006). In the assemblages from this group, 74 % are epifaunal (in which 55 % are miliolids), epiphytic, free-living, or attached (*A. problema, A. dividens, P. consobrina, V. rotunda*, etc) preferring oxic conditions and living in muddy to sandy sediment with marine to hypersaline water (see Table 1). However, 25 % are infaunal (*A. inflata*, *A. parkinsoniana, Ammonia beccarii, E. hauerinum,* etc.), which can tolerate occasional bottom anoxia and brackish waters (Murray 2006; Supplement). The second group (2; Fig. 4), excluding the overlap with the first group, is represented by the environment of hypersaline lagoons tolerating assemblages. The assemblage is dominated by epifaunal species (81 %), including miliolids (69 %). These species tolerate organic enrichment (*P. granosum*; Jorissen et al. 2018). However, *Q. akneriana*, for example, is considered sensitive to the increase of organic matter enrichment (Dimiza et al. 2016). They are also known for their high tolerance to salinity fluctuations and oxic/suboxic conditions. The remaining 19 % of species are infaunal or free living (*Cribroelphidium excavatum, Nonion* sp., *E. hauerinum, Elphidiella serena*, etc), preferring muddy and sandy sediment, from oxic-dysoxic conditions. Small group (3) characterizes the overlap between hypersaline shallow lagoonal – inner shelf environments and consists of only three samples with a majority (81 %) of epifaunal, epiphytic, and free-living foraminifera (e.g., *T. inflata, Quinqueloculina bogdanoviczi*, *Q. akneriana*, *Neoeponides schreibersii*, *P. consobrina*) and 19 % of infaunal (*A. parkinsoniana*, *Haynesina* sp.). The last group (4) represents a shelf environment with 66 % of epifaunal and epiphytic communities living in hyposaline conditions (e.g., *Porosononion* gr. *granosum*, *V. reussi, V. rotunda, Miliolinella selene*) along with 34 % infaunal and free-living (*A. viennensis, A. inflata, A. parkinsoniana, E. hauerinum*) taxa with adaptation to bottom anoxia (Langer 1988; Sen Gupta 2003; Murray 2006). A minor content of infaunal taxa in all identified groups can mirror the situation of accumulated assemblage from leaves (oxyphilic epifauna) and shallow infauna tolerating high nutrient and/or low oxi conditions of taxa inhabiting rhizomes of algae, or sea grasses and water/sediment interface (Langer 1988; Edgar 1999; Holcová & Zágoršek 2008).

Using PCA, we selected three sample-rich sample groups with different sample compositions (the following percentage is averaged for each group; Figs. 5, 6). The first group (MG 1) is defined by 50 % of infaunal species preferring muddy or sandy sediments, brakish-hypersaline lagoons, estuaries, and inner shelf with occasional suboxia/anoxia. The other 50 % (from which 19 % are EP-C) are epifaunal epiphytic species living in the arborescent algae that covers the bottom with an organic matter enriched environment (*P. granosum*). We can assume that the mentioned group of samples contains "third-order opportunistic species" with a high organic content (Dimiza et al. 2016; Jorissen et al. 2018; Bouchet et al. 2021). However, the present miliolid foraminifera are sensitive to the increase of organic matter enrichment (Table 1; Langer 1993). The second group (MG 2) is represented by over 67 % (from which 14 % are EP-C) of epifaunal species and epiphytes (*P. granosum*, *Q. akneriana*, *V. rotunda, P. consobrina*, *A. articulinoides*, *C. cristata*, etc.) possessing marine–hypersaline lagoons to the shelf. The remaining 33 % is characterized by infaunal communities (*A. parkinsoniana*, *A. beccarii*, *A. inflata*, *E. hauerinum*, *Valvulineria akneriana*, etc.) tolerating from brackish to hypersaline waters of brackish marshes–lagoons and the inner shelf. This group likely indicates an environment with lowered salinity and potential oxygen depletion at the bottom. The third (MG 3) group is represented by significant dominance (97 %) of epifaunal epiphytic

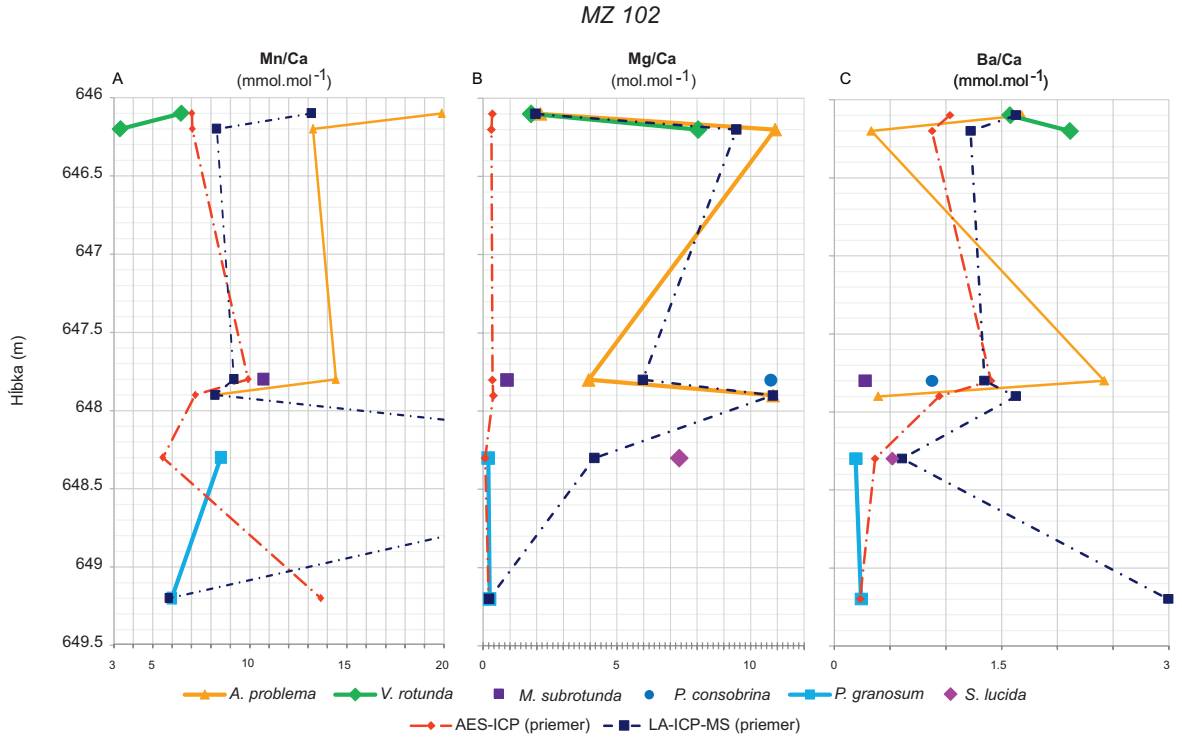

Fig. 8. Stratigraphic changes in Mn/Ca, Mg/Ca, and Ba/Ca compositions of foraminifera shells from borehole *MZ102*.

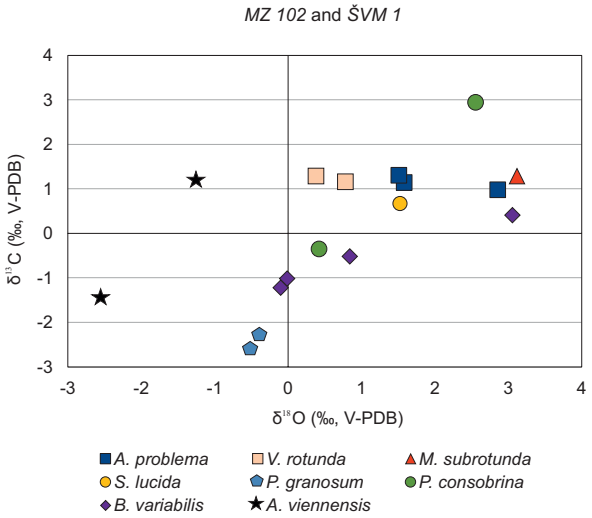

Fig. 9. Oxygen isotope and carbon isotope variations of foraminifera from *MZ102* (*A. problema*, *S. lucida*, *V. rotunda*, *M. subrotunda*, *P. consobrina* and *P. granosum*) and *ŠVM1* (*B. variabilis* and *A. viennensis*).

species (*Q. akneriana*, *A. problema*, *P. consobrina*, *A. articulinoides*, *V. rotunda*, *M. subrotunda*, etc.) living in marine–hypersaline shallow lagoons to inner shelf preferring oxic conditions. One of the smaller groups (SG 1) is interpreted as 73 % epifaunal (EP-D 29.8 %, EP-B+A 23 %, EP-C 20 %) particularly *P. subgranosus*, *P. consobrina*, and infaunal *E. serena* and *Bolivina moldavica*, which indicates an inner shelf marine environment (Goubert et al. 2001; Keen 2004; Gildeeva et al. 2021). *P. subgranosus* with *P. consobrina* tolerate oxygen-rich environments in the inner shelf and normal marine to hypersaline lagoons with a probable occurrence of plant substrates; however, the present infauna indicates occasional bottom water dysoxia (Murray 2006). The second small group (SG 2), which contains only three samples from *Machów*, is characterized by a high percentage (75 %) of epifaunal epiphyte (EP-B+A), *A. dividens* and *L. lobatula.* Together with small miliolids (EP-D 24 %), these highly-diversified communities describe shallow marine conditions.

Stable isotopes and element/calcium ratios in foraminifera shells

Light $\delta^{18}O$ measurements (Table 3) from the Danube Basin, *B. variabilis* and *A. viennensis* (173–173.2 m) from *ŠVM1*, and from the Vienna basin, *P. granosum* (648.3–649.2) from *MZ102*, could represent a shallow water environment and low salinity with possible warm river water inflow (Gonera et al. 2000), which could be correlated with the higher Ba/Ca and lower Mg/Ca values in *MZ102*. Foraminifera assemblages confirm lower salinity as well (Figs. 7, 8).

Positive $\delta^{18}O$ values of miliolids from *MZ102* (647.8–647.9 m) could be related to the warmer (tropical) temperature around ~27–30 °C (Boltovskoy & Wright 1976) and high salinity because of stress conditions, and/or because of isolation from other basins of the Paratethys (Seneš 1961a, b; Popov et al. 2004; Báldi 2006; Piller et al. 2007; Gozhyk et al.

2015; Neubauer et al. 2015; Kováč et al. 2017a,b). This hypothesis is also supported by the Mg/Ca and Ba/Ca ratios, where the values rapidly changed with increasing depth. Lower, but still positive values of oxygen isotope ratios of miliolids (646.1–646.2 and 648.3 m) could represent an environment with warm-temperate temperature (~17–22 °C). If we consider that for every 1.2 ‰ increase in seawater $\delta^{18}O$, salinity increases by 10 ‰ (as proposed by Shackleton 1987), we hypothesize that the $\delta^{18}O$ difference towards the base represents a salinity decrease of ~10 ‰. This is also supported by the Mg/Ca and Ba/Ca ratios; however, the entire section (646.1–648.3 m) manifests high fluctuations in salinity (Fig. 8b,c).

Salinity fluctuations were considered a reason for the Sarmatian extinction of molluscs and foraminifera fauna (Piller & Harzhauser 2005; Holcová 2008). Our results show observable shifts in the representation of miliolid species (Fig. 8b,c). During the early Sarmatian, the water was predominantly shallow and oligotrophic, quite possibly a few metres deep (<100 m) as we can interpret from the dominant epiphytic faunal composition of the associations. Salinity in the central parts of the basins in the Central Paratethys was mainly normal marine, while in the lower Sarmatian sediments, it tended more towards brackish to marine, with episodes of hypersalinity (Piller & Harzhauser 2005; Filipescu & Silye 2008; Tóth et al. 2010; Zlinská et al. 2010; Bitner et al. 2014; Ruman et al. 2017), which is also shown in our results, where samples are grouped along the salinity and oxygen as main influencing factors (Figs.7, 8).

The $\delta^{13}C$ results derived from the foraminiferal shell analysis indicate the presence of organic matter input, primarily originating from river sources (Berger 1981); a riverine deltaic environment is documented in the studied sediments from the *ŠVM 1* borehole (Kováč et al. 2008). Typically, a depletion of $\delta^{13}C$ is observed in bottom water, leading to lower values in the foraminiferal shells (Naidu & Niitsuma 2004). On the other hand, symbiont-bearing foraminifera tend to display positive $\delta^{13}C$ values in their shells due to photosynthetic processes. These symbionts utilize more $^{12}CO_2$, resulting in an elevation of $\delta_{13}C$ within the foraminifera shells (Spero & Lea 1993). The positive $\delta^{13}C$ values (*A. viennensis*, *S. lucida*, *A. problema*, *N. subrotunda*, *P. consobrina*) observed in our results (*MZ 102,* depth from 646.1 to 648.3) are likely influenced by a life position in pore water (Grossman 1984), or, as seen from our results, a possible higher position at the vegetation (Table 1) level with varying temperature and pH. Conversely, the negative $\delta^{13}C$ values recorded in the *MZ 102* (depth 648.3–649.2) and *ŠVM 1* samples may be attributed to increasing carbon derived from the decomposition of isotopically-light organic matter into the pore water. This is further supported by the presence of benthic species, such as *Bulimina*, *Porosononion*, and *Ammonia*, which are shallow infaunal and thus indicative of oxygen-deficient conditions (Dimiza et al. 2016; Jorissen et al. 2018; Bouchet et al. 2021).

Our results, which were evaluated by traditional taxonomic methods and the morphogroup approach, correspond to the results from the geochemical study of their tests (Figs. 8, 9, 10). Association documented higher salinity in the depths of 646.2 m and 647.8 m (*MZ 102* borehole), as well as yields of foraminifera shells (miliolids and hyaline as well) with high Mg/Ca and low Ba/Ca signal. The barium concentrations in foraminifera calcite (Ba/Ca) increase when salinity decreases (Hall & Chan 2004; Weldeab et al. 2007; Bahr et al. 2013; Groeneveld et al. 2018), which is in inverse relation to the salinity and Mg/Ca concentrations. Several other studies suggest that increasing benthic foraminifera Mg/Ca can also be used as a salinity proxy (e.g., Tóth et al. 2010; Groeneveld & Filipsson 2013; Groeneveld et al. 2018). The Mn/Ca in the foraminifera shells reflects the amount of dissolved oxygen in the surrounding water in which they lived – with decreasing oxygen, the manganese ratio increases (Froelich et al. 1979; Burdige 1993; Calvert & Pedersen 1993; Canfield et al. 1993; Tribovillard et al. 2006). The analysis of the shells collected from the borehole *MZ 102* (646.1–649.2 m) documents changes of the dissolved oxygen in the water column (Figs. 7 and 8a). The samples with the higher Mn/Ca (depth 646.1–646.2 m, 648.3 m) are in correlation with the IAE and taxonomy results, showing suboxic to dysoxic conditions.

Paleoenvironments

The large symbiont bearing miliolids, such as *Borelis* or *Peneroplis*, are documented only from the Badenian MH sediments in our study (Table 2), suggesting the change of miliolide assemblages at the Badenian/Sarmatian boundary, where Badenian MH contained a higher amount of EP-C (Figs. 5, 6). Nevertheless, MH are developed in both the Badenian and Sarmatian sediments; however, in the Sarmatian, they are more frequent (31 MH; Table 2, Fig. 6). The paleontological interpretation relied on a comprehensive approach that incorporated taxonomy, morphogroup division, and geochemical analyses, including isotopic and element/Ca composition assessments of foraminifera shells. The study of miliolid dominated associations (MH) revealed the presence of three main (MG 1, 2, 3) and two small (SG 1, 2) groups using PCA representing specific microhabitats as illustrated in Figure 11. The difference between major (MG 1, 2, 3) and small groups (SG 1, 2) is in the more open marine environment documented by the presence of oxyphilic species and higher foraminifera diversity. The floral associations for each group are taken from the work of Langer (1993).

MG 1 – This group inhabits brackish to hypersaline lagoons, estuaries, and inner shelves. These habitats are characterized by the presence of infaunal and epifaunal-epiphytic communities, often referred to as 'third-order opportunistic species.' These communities are typically associated with microhabitats – specific faunal communities, particularly those harboured on arborescent algae, such as *Cutleria* and *Fucus*. The notable presence of high detrital content in the water substrates occasionally leads to bottom water suboxia or anoxia in muddy–sandy sediment layers.

MG 2 – The second group's analysis pertains to a broad spectrum of habitats ranging from shallow marine environments to hypersaline lagoons, where salinity levels exhibit notable fluctuations. Within these environments, a distinctive association is observed, characterized by infaunal, and small epiphytic, motile species. They are typically found in close proximity to short-stemmed arborescent algae such as *Padina, Halopteris*, and *Pseudolithophyllum*. The presence of detrital content on the seabed may result in potential oxygen depletion in the sediment below, resulting in suboxic conditions.

MG 3 – The third environment exhibits a faunal composition corresponding to shallow marine-hypersaline, hypersaline lagoons, and the inner shelf. Within these habitats, the faunal association is characterized by the substantial presence of permanently motile epiphytic foraminifera climbing on stems and/or rhizomes. These communities live within floral associations of *Padina*, *Halopteris*, *Pseudolithophyllum*, and *Posidonia* rhizomes. The water bodies within this group maintain a well-oxygenated state. Sediment can vary from muddy to muddy with boulders, but predominantly a hard and rocky substrate. Despite the generally oxygen-rich conditions, the presence of shallow infauna indicates occasional occurrences of anoxic conditions.

SG 1 – This small group indicates marine environments within the inner shelf, occasionally experiencing open marine conditions. The foraminifera association within this group is characterized by a diverse microfauna compromising both infaunal and all categories of epiphytic species. They live among a variety of flora, including *Padina*, *Halopteris*, *Pseudolithophyllum*, *Posidonia*, and *Sargassum*, contributing to the intricate ecological balance of these habitats. While the water column generally maintains a well-oxygenated state, the large amount of shallow infauna suggests occasional anoxic conditions.

SG 2 – The final group characterizes marine inner shelf environments, occasionally transitioning the open marine conditions. Within this setting, highly diversified fauna thrives and is represented by the abundant presence of motile epiphytic species, thus inhabiting the intricate meshwork of filamentous algal blades of *Posidonia* and *Sargassum*. The water within this environment maintains a consistent, well-oxygenated state, with a deeper water column and well-oxygenated sediment.

Conclusions

The multiproxy approach of miliolid-rich assemblages' studies across various middle Miocene Serravallian (Badenian/Sarmatian) localities within the Central Paratethys region reveals significant environmental variations. These paleoenvironments were identified predominantly in the upper Badenian and Sarmatian sediments and are represented by a diverse array of habitats ranging from brackish–normal marine and hypersaline shallow lagoons, as well as estuaries and inner shelves, which occasionally transition to open marine

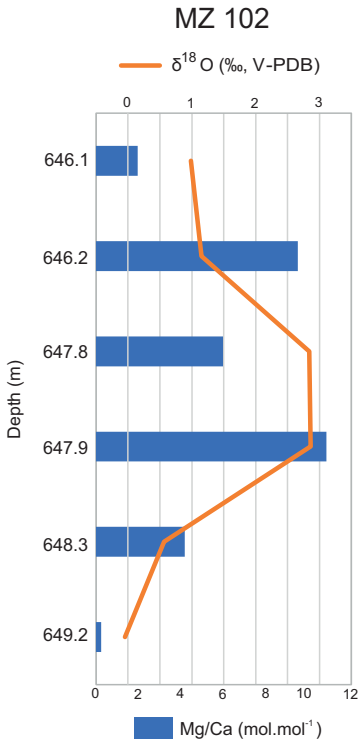

Fig. 10. Comparison of Mg/Ca and $\delta^{18}O$ data of foraminifera from *MZ 102*.

conditions (Figs. 6, 11). The MHs were found in four Badenian levels and 31 MHs were identified in Sarmatian sediments. The main difference between the Badenian and Sarmatian MHs is the absence of large symbiont bearing foraminifers in Sarmatian sediments. Foraminifera associations analysis alongside geochemical data indicates dynamic and fluctuating marginal marine environment. Assemblages depend on (1) Substrate (muddy/sandy to hard), (2) nutrient content, (3) oxygen content and (4) salinity. The environments identified here are marked by instability and a strong presence of vegetation, which indicative of high salinity fluctuations. Moreover, evidence suggests river influxes contributing to changes in water temperature. Finally, the presence of a high detrital content within these habitats underscores the occasional occurrence of bottom suboxia or even anoxia.

MH from Badenian sediments (*Machów*) of the Carpathian Foredeep indicate a deeper water environment with seagrass cover and/or possibly a rocky substrate. In contrast, associations typical of brackish or hypersaline lagoons, estuaries, and the inner shelf, which is occasionally depleted of oxygen content in the sediment, were found in the Badenian sediments of the western margin of the Paratethys (*Poddvorov 96, Poddvorov 118*).

The samples from the Sarmatian sediments revealed a greater diversity of marginal marine environments with specific sedimentary conditions (Fig. 6). The most prominent feature is the fluctuation of salinity, which is likely caused by a lowering of the sea level and the influx of river water,

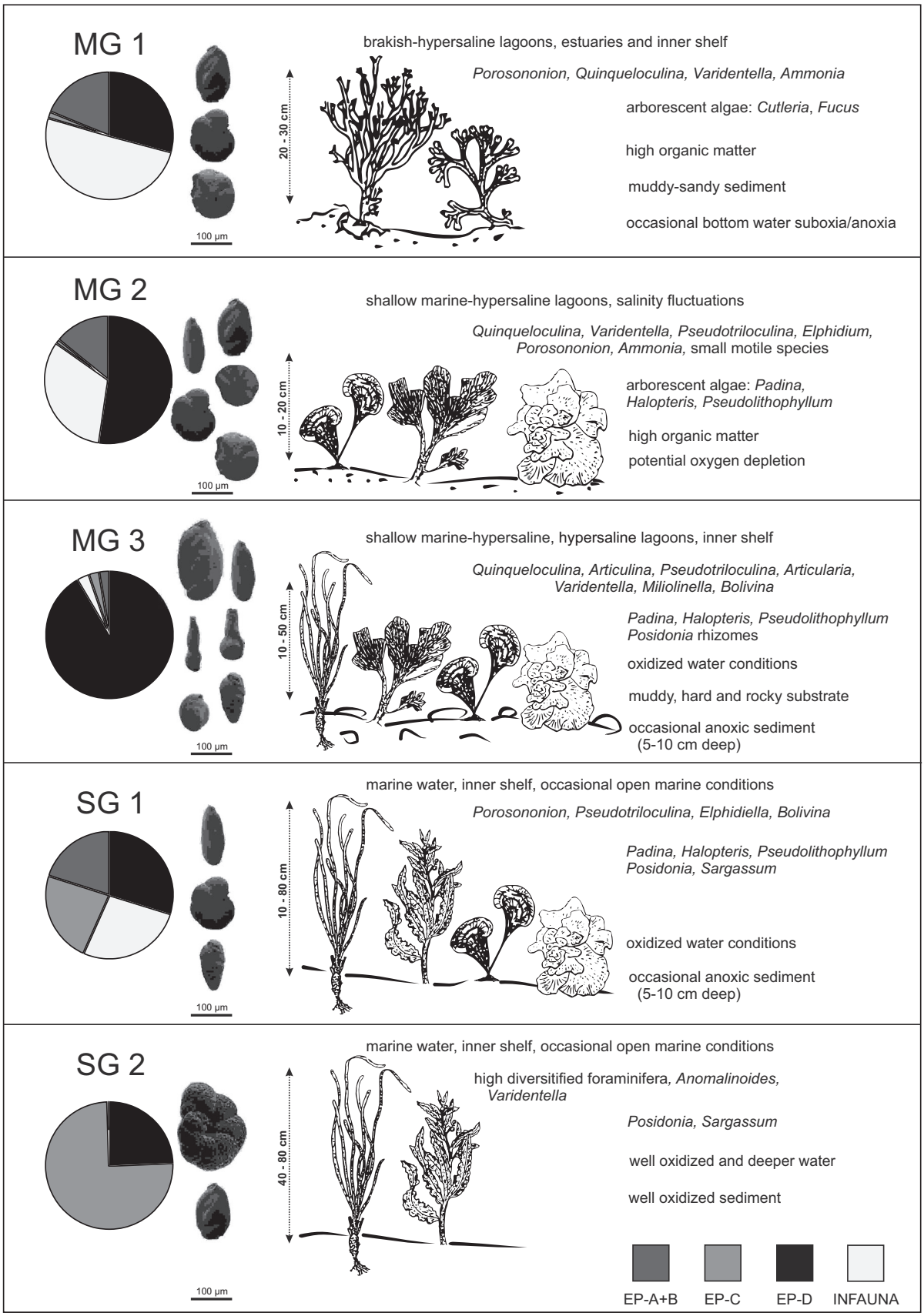

Fig. 11. Reconstruction of paleoenvironments and paleobiotopes dominated by small miliolids (MH) during the Middle Miocene according to this study. Explanatory notes: MG 1, 2, 3 – main groups 1, 2 and 3; SG 1, 2, 3 – small groups 1 and 2.

depending on the paleogeography of the area. In the eastern part of the Carpathian Foredeep (*Rădăuţi* and *Dorneşti*), on its western margin, shallow water environments were identified with varying salinity levels (MG 1–3), and a freshwater influx is also assumed (MG 1). At the *Costeşti* site, normal marine to hypersaline environments with muddy, sandy, to rocky substrates were identified (MG 2, 3). In the easternmost part (*Tuğlu*), the environment was defined as exclusively hypersaline (MG 3). The northern edge of the studied area (*Machów* and *Jamnica M83*) is characterized by the greatest environmental variability (all paleoenvironmental groups), typical of dynamic changes in paleogeographic and paleoclimatic conditions on the margin of the sedimentary space. The western edge of the studied area is defined by shallow water environments, which differ in salinity and substrate content (MG 1–3; SG 1), at sites such as the Malacky reservoir, *Suchohrad 63*, *Rohožník 112*, *ŠVM 1*, and *Ivanka 1*. These differ from the previous sites due to the reduced oxygen content in the bottom water and substrate.

Acknowledgments: This study was supported by the projects: APVV-20-0079, APVV-20-0120, and VEGA 2/0013/20, VEGA-2/0169/19.

References

Abdul Aziz H., Di Stefano A., Foresi L.M., Hilgen F.J., Iaccarino S.M., Kuiper K.F., Lirer F., Salvatorini G. & Turco E. 2008: Integrated stratigraphy and $^{40}Ar/^{39}Ar$ chronology of early Middle Miocene sediments from DSDP Leg 42A, Site 372 (Western Mediterranean). *Palaeogeography, Palaeoclimatology, Palaeoecology* 257, 123–138. https://doi.org/10.1016/j.palaeo.2007.09.013

Andrejeva Grigorovič A.S., Kováč M., Halásová E. & Hudáčková N. 2001: Litho and Biostratigraphy of the Lower and Middle Miocene sediments of the Vienna basin (NE part) on the basis of calcareous nannoplankton and foraminifers. *Scripta Facultatis Scientiarum Naturalium Universitatis Masarykianae Brunensis, Geology* 30, 23–27.

Babejová-Kmecová J. 2020: Spoločenstvá dierkavcov s prevahou zástupcov čeľade Miliolidae v neogénnych sedimentoch Centrálnej Paratetýdy. *Diploma thesis, Comenius University in Bratislava*, Bratislava, 1–84.

Babejová-Kmecová J., Plašienková I., Sliva Ľ., Halásová E. & Hudáčková N. 2022: From dysoxic sea to hypersaline lagoon: paleoenvironmental changes on the Badenian/Sarmatian boun-dary (borehole MZ 102; Vienna Basin*). Acta Geologica Slovaca* 14, 57–72.

Bahr A., Schönfeld J., Hofmann J., Voigt S., Aurahs R., Kucera M., Flögel S., Jentzen A., & Gerdes A. 2013: Comparison of Ba/Ca and $\delta^{18}O_{water}$ as freshwater proxies: A multi-species core-top study on planktonic foraminifera from the vicinity of the Orinocohttps River mouth. *Earth and Planetary Science Letters* 383, 45–57. https://doi.org/10.1016/j.epsl.2013.09.036

Báldi T. 1980: The early History of the Paratethys. *Földtani Közlöny* 110, 456–472 (in Hungarian with English summary).

Báldi K. 2006: Paleoceanography and climate of the Badenian (Middle Miocene, 16.4–13.0 Ma) in the Central Paratethys based on foraminifera and stable isotope ($\delta^{18}O$ and $\delta^{13}C$) evidence. *International Journal of Earth Science (Geologische Rundschau)* 95, 119–142. https://doi.org/10.1007/s00531-005-0019-9

Baráth I., Kováč M., Soták J. & Lankreijer A. 1997: Tertiary collision, metamorphism and basin forming processes in the Eastern Slovakia (central Western Carpathians). In: Grecula P., Hovorka D. & Putiš M. (Eds.): Geological Evolution of the Western Carpathians. *Mineralia slovaca – Monograph*, 65–78.

Berger W.H. 1981: Oxygen and carbon isotopes in foraminifera: an introduction. In: Berger W.H., Bé A.W.H. & Vincent E. (Eds.): Oxygen and Carbon Isotopes in Recent Foraminifera (Symposium). *Palaeogeography, Palaeoclimatology, Palaeoecology* 33, 3–7.

Bitner M.A., Zágoršek K., Halásová E., Hudáčková N. & Jamrich M. 2014: Brachiopods and bryozoans from the Sandberg section (Vienna Basin, Central Paratethys) and their significance for environmental interpretation of the Early Sarmatian (= Middle Miocene) Sea. *Neues Jahrbuch für Geologie und Paläontologie Abhandlungen* 273, 207–219. https://doi.org/10.1127/0077-7749/2014/0424

Boltovskoy E. & Wright R. 1976: Recent Foraminifera. xvii + 515 pp., 133 s, 17 tables. Junk, The Hague. Price Dutch Guilders 125.00. *Geological Magazine* 114, 158. https://doi.org/10.1017/s0016756800044332

Bouchet V., Frontalini F., Francescangeli F., Sauriau P., Geslin E., Almogi-Labin A., Avnaim-Katav S., Bella L., Cearreta A., Coccioni R., Costelloe A., Dimiza M., Ferraro L., Haynert K., Martinez-Colon M., Melis R. Schweizer M., Triantaphyllou M., Tsujimoto A. & Martins M.V. 2021: Indicative value of benthic foraminifera for biomonitoring: Assignment to ecological groups of sensitivity to total organic carbon of species from European intertidal areas and transitional waters. *Marine Pollution Bulletin* 164, 112071. https://doi.org/10.1016/j.marpolbul.2021.112071

Burdige D.J. 1993: The biogeochemistry of manganese and iron reduction in marine sediments. *Earth-Science Reviews* 35, 249–284.

Calvert S.E. & Pedersen T.F. 1993: Geochemistry of Recent Oxic and Anoxic Marine Sediments: Implications for the Geological Record. *Marine Geology* 113, 67–88. https://doi.org/10.1016/0025-3227(93)90150-T

Canfield D.E., Thamdrup B. & Jansen J.W. 1993: The anaerobic degradation of organic matter in Danish coastal sediments: Iron reduction, manganese reduction, and sulphate reduction. *Geochimica et Cosmochimica Acta* 57, 3867–3883.

Cicha I., Čtyroká J., Jiříček R. & Zapletalová I. 1975: Principal biozones of the Late Tertiary in the East Alps and West Carpathians. In: Cicha I. (Ed.): Biozonal division of the Upper Tertiary basins of the Eastern Alps and West Carpathians. IUGS Proceedings of the VI Congress Bratislava. *Geological survey*, Prague, 19–34.

Cicha I., Rögl F., Rupp Ch. & Čtyroká J. (Eds.) 1998: Oligocene–Miocene foraminifera of the Central Paratethys. *Abhandlungen der Senckenbergischen Naturforschenden Gesellschaft* 549, 1–325.

Čierna E. 1974: Mikropalaontologishe und biostratigrapische untersuchung einiger bohrproben aus der weiteren umgebung von Rohožník. *Acta Geographica Universitatis Comenianae, Geologica,* Bratislava, 113–187.

Dimiza M.D., Triantaphyllou M.V., Koukousioura O., Hallock P., Simboura N., Karageorgis A.P., Papathanassiou E. 2016: The Foram Stress Index: A new tool for environmental assessment of soft-bottom environments using benthic foraminifera. A case study from the Saronikos Gulf, Greece, Eastern Mediterranean. *Ecological Indicators* 60, 611–621. https://doi.org/10.1016/j.ecolind.2015.07.030

Dubicka Z., Złotnik M. & Borszcz T. 2015: Test morphology as a function of behavioral strategies – Inferences from benthic foraminifera. *Marine Micropaleontology* 116, 38–49. https://doi.org/10.1016/j.marmicro.2015.01.003

Dumitriu S.D., Loghin S., Dubick Z., Melinte-Dobrinescu, M.C., Paruch-Kulczycka J. & Ionesi V. 2017: Foraminiferal, ostracod, and calcareous nannofossil biostratigraphy of the latest Badenian–Sarmatian interval (Middle Miocene, Paratethys) from Poland, Romania and the Republic of Moldova. *Geologica Carpathica* 68, 419–444. https://doi.org/10.1515/geoca-2017-0028

Dumitriu S.D., Dubicka Z. & Ionesi V. 2018: The functional significance of the spinose keel structure of benthic foraminifera: inferences from *Miliolina cristata* Millett, 1898 (Miliolida) from northeast Romania. *Journal of Micropalaeontology* 37, 153–166. https://doi.org/10.5194/jm-37-153-2018

Dumitriu S.D., Dubicka Z., Loghin S., Melinte-Dobrinescu C. & Paruch-Kulczyca J. 2020: The evolution of the Carpathian Foredeep Basin during the latest Badenian and Sarmatian (middle Miocene): inferences from micropalaeontological data. *Geological Quarterly* 64, 1004–1022. https://doi.org/10.7306/gq.1568

Edgar G.J. 1999: Experimental analysis of structural versus trophic importance of seagrass beds. In: Effects on macrofaunal and meiofaunal invertebrates. *Vie et Milieu / Life & Environment*, 239–248.

Epstein S., Buchsbaum R., Lowenstam H.A. & Urey H.C. 1953: Revised carbonate-water isotopic temperature scale, *Geological Society of America Bulletin* 64, 1315–1325.

Filipescu S. & Silye L. 2008: New paratethyan biozones of planktonic foraminifera described from the Middle Miocene of the Transylvanian Basin (Romania). *Geologica Carpathica* 59, 537–544.

Froelich P.N., Klinkhammer G.P., Bender M.L., Luedtke N.A., Heath G.R., Cullen D., Dauphin P., Hammond D., Hartman B. & Maynard V. 1979: Early oxidation of organic matter in pelagic sediments of the eastern equatorial Atlantic: suboxic diagenesis. *Geochimica et Cosmochimica Acta* 43, 1075–1090.

Fuksi T. 2015: Multivariate paleoecological analyses of Badenian and Sarmatian molluscan assemblages from the NW ViennaBasin (Rohožník-Konopiská, Slovakia). *Geology, Geophysics and Environment* 41, 80–81. https://doi.org/10.7494/geol.2015.41.1.80

Galović I. & Young J. 2012: Revised taxonomy and stratigraphy of Middle Miocene calcareous nannofossils of the Paratethys. *Micropaleontology* 58, 305–334.

Gildeeva O., Akita L.G., Biehler J., Frenzel P. & Alivernini M. 2021: Recent brackish water Foraminifera and Ostracoda from two estuaries in Ghana, and their potential as (palaeo) environmental indicators. *Estuarine, Coastal and Shelf Science* 256, 107–270

Gonera M., Peryt T.M. & Durakiewicz T. 2000: Biostratigraphical and palaeoenvironmental implications of isotopic studies (^{18}O, ^{13}C) of Middle Miocene (Badenian) foraminifers in the Central Paratethys. *Terra Nova* 12, 231–238.

Goubert E., Néraudeau D., Rouchy J.M. & Lacourt D. 2001: Foraminiferal record of environmental changes: Messinian of the Los Yesosarez (Sorbas Basin, SE Spain). *Palaeogeography, Palaeoclimatology, Palaeoecology* 175, 61–78. https://doi.org/10.1016/S0031-0182(01)00386-8

Gozhyk P., Semenenko V., Andreeva-Grigorovich A. & Maslun N. 2015: The correlation of the Neogene of Central and Eastern Paratethys segments of Ukraine with the International Stratigraphic Chart based on planktonic microfossils. *Geologica Carpathica* 66, 235–244. https://doi.org/10.1515/geoca-2015-0022

Gradstein F.M., Ogg, J.G. & Hilgen F.J. 2012: On the geologic time scale. *Newsletters on Stratigraphy* 45, 171–188. https://doi.org/10.1127/0078-0421/2012/0020

Grill R. 1941: Stratigraphische Untersuchungen mit Hilfe von Mikrofaunen im Wiener Becken und den benachbarten Molasse-Anteilen. *Oel und Kohle* 37, 595–602.

Grill R. 1943: Über mikropaläontologische Gliederungsmöglichkeiten im Miozän des Wiener Beckens. *Mitteilungen des Reichsamts für Bodenforschung* 6, 33–44.

Groeneveld J. & Filipsson H.L. 2013: Mg/Ca and Mn/Ca ratios in benthic foraminifera: the potential to reconstruct past variations in temperature and hypoxia in shelf regions. *Biogeosciences* 10, 5125–5138. https://doi.org/10.5194/bg-10-5125-2013

Groeneveld J., Filipsso H.L., Austin W.E., Darling K., McCarthy D., Quintana Krupinski N.B., et al. 2018: Assessing proxy signatures of temperature, salinity, and hypoxia in the Baltic Sea through foraminifera-based geochemistry and faunal assemblages. *Journal of Micropalaeontology* 37, 403–429. https://doi.org/10.5194/jm-37-403-2018

Grossman E.L. 1984: Carbon isotopic fractionation in live benthic foraminifera – comparison with inorganic precipitate studies. *Geochimica et Cosmochimica Acta* 48, 1505–1512.

Hall J.M. & Chan L.H. 2004: Li/Ca in multiple species of benthic and planktonic foraminifera: Thermocline, latitudinal, and glacial–interglacial variation. *Geochimica et Cosmochimica Acta* 68, 529–545. https://doi.org/10.1016/S0016-7037(03)00451-4

Hallock P. 1988a: Interoceanic differences in foraminifera with symbiotic algae: A result of nutrient supplies? *Proceedings of the 6th International Coral Reef Symposium, Australia* 3, 5–251.

Hallock P. 1988b: Diversification in algal symbiont bearing foraminifera: A response to oligotrophy? *Revue de Paléobiologie, Volume Spécial* 2, 97–789.

Hammer Ø., Harper D.A.T. & Ryan P.D. 2001: PAST: Paleontological Statistics Software Package for Education and Data Analysis. *Palaeontologia Electronica* 4, 4.

Harzhauser M. & Piller W.E. 2007: Benchmark data of a changing sea – Palaeogeography, Palaeobiogeography and events in the Central Paratethys during the Miocene. *Palaeogeography, Palaeoclimatology, Palaeoecology* 253, 8–31. https://doi.org/10.1016/j.palaeo.2007.03.031

Harzhauser M., Piller W.E. & Steininger F.F. 2002: Circum-Mediterranean Oligo–Miocene biogeographic evolution – the gastropods' point of view. *Palaeogeography, Palaeoclimatology, Palaeoecology* 183, 103–133. https://doi.org/10.1016/S0031-0182(01)00464-3

Hohenegger J. 2011: Large foraminifera, Greenhouse constructions and gardeners in the oceanic microcosmos. *The Kagoshima University museum*, Kagoshima, 1–81.

Hohenegger J., Coric S. & Wagreich M. 2014: Timing of the middle miocene badenian stage of the central paratethys. *Geologica Carpathica* 65, 55–66. https://doi.org/10.2478/geoca-2014-0004

Holcová K. 2008: Foraminiferal species diversity in the Central Paratethys – a reflection of global or local events? *Geologica Carpathica* 59, 71–85.

Holcová K. & Zágoršek K. 2008: Bryozoa, foraminifera and calcareous nannoplankton as environmental proxies of the "bryozoan event" in the Middle Miocene of the Central Paratethys (Czech Republic), *Palaeogeography, Palaeoclimatology, Palaeoecology* 267, 216–234. https://doi.org/10.1016/j.palaeo.2008.06.019

Hudáčková N. & Keblovská Z. 2012: Záverečná správa z mikropaleontologického vyhodnotenia vrtných jadier vrtov Podd.126, Podd.106, Podd.102, Podd.101, Podd.96, Podd.95. *Záverečné správy*. *Nafta a.s.*, 1–28 (in Slovak).

Hudáčková N., Grigorovič A.S.D & Halásová, E. 2001: Biostratigrafické vyhodnotenie jadier vrtov Ložín 1, Albinov 4 a Iňačovce 3. *Katedra geológie a paleontológie, Prírodovedecká fakulta Univerzity Komenského*, Bratislava, 1–17.

Hudáčková N., Sliva, Ľ., Halásová, E. & Pipík R. 2004: Sedimentologické, biostratigrafické a paleontologické vyhodnotenie jadra vrtu Su–63 (Suchohrad). *Katedra geológie a paleontológie, Prírodovedecká fakulta Univerzity Komenského*, Bratislava, 1–31.

Hudáčková N., Halásová E., Koubová I. & Kováčová M. 2009: From the deep marine to shallow water paleoenvironment of the Upper Badenian to Sarmatian sediments (Slovak part of the Vienna Basin). In: Németh Z., Plašienka D., Šimon L., Kohút M. & Iglárová Ľ. (Eds.): 8th Annual Seminary of the Slovak Geological Society. *Mineralia Slovaca* 41, 547–548.

Hudáčková N., Holcová K., Halásová E., Kováčová M., Doláková N., Trubač J., Rybár S., Ruman A., Starek D., Šujan M., Jamrich M. & Kováč M. 2020: The Pannonian Basin System northern margin paleogeography, climate, and depositional environments in the time range during MMCT (Central Paratethys, Novohrad–Nograd Basin, Slovakia). *Palaeontologia Electronica* 23, a50. https://doi.org/10.26879/1067

Il'ina L.B. 2000: On connections between basins of the Eastern Paratethys and adjacent seas in the middle and late Miocene. *Stratigraphy and Geological Correlation* 8, 300–305.

Ionesi B. 1991: The biozonation of the Sarmatian from the Moldavian platform [Biozonarea sarmaţianului din platforma moldovenească]. In: The celebration days of Alexandru Ioan Cuza University of Iasi, 25–26 (in Romanian).

Jorissen F.J., Nardelli M.P., Almogi-Labin A., Barras C., Bergamin L., Bicchi E., ElKateb A., Ferraro L., McGann M., Morigi C., Romano E., Sabbatini A.,Schweizer M. & Spezzaferri S. 2018: Developing Foram-AMBI for biomonitoring in the Mediterranean: species assignments to ecological categories. *Marine Micropaleontology* 140, 33–45. https://doi.org/10.1016/j.marmicro.2017.12.006

Kaiho K. 1991: Global changes of Paleogene aerobic/anaerobic benthic foraminifera and deep-sea circulation. *Palaeogeography, Palaeoclimatology, Palaeoecology* 83, 65–85.

Kaiho K. 1999: Effect of organic carbon flux and dissolved oxygen on the benthic foraminiferal oxygen index (BFOI). *Marine Micropaleontology* 37, 67–76.

Keen M.C. 2004: The origin of the modern tropical West African marine Ostracod Fauna, with a description of the Ruggieriini n. tribe. *Bollettino della Societa Paleontologica Italiana* 43, 201–216.

Kilényi E. & Šefara J. (Eds.) 1989: Pre-Tertiary basement contour map of the Carpathian Basin beneath Austria, Czechoslovakia and Hungary, 1:500,000. *Eötvös Lóránd Geophysical Institute*, Budapest.

Koubová I. & Hudáčková N. 2010: Foraminiferal successions in the shallow water Sarmatian sediments from the MZ 93 borehole (Vienna Basin, Slovak part). *Acta Geologica Slovaca* 2, 47–58.

Kováč M. 2000: Geodynamický, paleogeografický a štruktúrny vývoj Karpatsko-Panónskeho regiónu v miocéne: Nový pohľad na neogénne panvy Slovenska [Geodynamic, palaeogeographic and structural development of the Carpatho-Pannonian region during the Miocene: new view on the Neogene basins of Slovakia]. *VEDA, SAV*, Bratislava, 1–202 (in Slovak).

Kováč M. & Zlinská A. 1998: Changes of paleoenvironment as a result of interaction of tectonic events and sea level oscillation in the East Slovakian Basin. *Przegląd Geologiczny* 46, 403–409.

Kováč M., Hudáčková N., Rudinec R. & Lankreijer A. 1996: Basin evolution in the foreland and hinterland of the Carpathian accretionary prism during the Neogene: evidence from the Western to Eastern Carpathians Junction. *Annales Tectonicae* 10, 3–19.

Kováč M., Baráth I. & Nagymarosy A. 1997: The Miocene collapse of the Alpine–Carpathian–Pannonian junction – an overview. *Acta Geologica Hungarica* 40, 241–264.

Kováč M., Baráth I., Harzhauser M., Hlavatý I. & Hudáčková N. 2004: Miocene depositional systems and sequence stratigraphy of the Vienna Basin. *Courier Forschungsinstitut Senckenberg* 246, 187–212.

Kováč M., Andreyeva-Grigorovich A., Bajraktarević Z., Brzobohatý R., Filipescu S., Fodor L., Harzhauser M., Nagymarosy A., Oszczypko N., Pavelić D., Rögl F., Saftić B., Sliva Ľ. & Studencka B. 2007: Badenian evolution of the Central Paratethys Sea: paleogeography, climate and eustatic sea-level changes. *Geologica Carpathica* 58, 579–606.

Kováč M., Andrejeva-Grigorovič A., Baráth I., Beláčková K., Fordinál K., Halásová E., Hók J., Hudáčková N., Chalupová B., Kováčová M., Sliva Ľ. & Šujan M. 2008: Litologické, sedimentologické a biostratigrafické vyhodnotenie vrtu ŠVM-1 Tajná [Lithologic, sedimentologic and biostratigraphic evaluation of the ŠVM-1 Tajná borehole]. *Geologické práce, Správy* 114, 51–84 (in Slovak with English abstract).

Kováč M., Hudáčková N., Halásová E., Kováčová M., Holcová K., Oszczypko-Clowes M., Báldi K., Less G., Nagymarosy A., Ruman A., Klučiar T. & Jamrich M. 2017a: The Central Paratethys palaeoceanography: a water circulation model based on microfossil proxies, climate, and changes of depositional environment. *Acta Geologica Slovaca* 9, 75–114.

Kováč M., Márton E., Oszczypko N., Vojtko R., Hók J., Králiková S., Plašienka D., Klučiar T., Hudáčková N. & Oszczypko-Clowes M. 2017b: Neogene palaeogeography and basin evolution of the Western Carpathians, Northern Pannonian domain and adjoining areas. *Global Planetary Change* 155, 133–154.

Kováčová P. & Hudáčková N. 2009: Late Badenian foraminifers from the Vienna Basin (Central Paratethys): stable isotope study and paleoecological implications. *Geologica Carpathica* 60, 59–70. https://doi.org/10.2478/v10096-009-0006-3

Kováčová P., Emmanuel L., Hudáčková N. & Renard M. 2009: Central Paratethys paleoenvironment during the Badenian (Middle Miocene): evidence from foraminifera and stable isotope ($\delta^{13}C$ and $\delta^{18}O$) study in the Vienna Basin (Slovakia). *International Journal of Earth Sciences* 98, 1109–1127. https://doi.org/10.1007/s00531-008-0307-2

Kranner M., Harzhauser M., Mandic O., Strauss P., Siedl W. & Piller W.E. 2021a: Early and middle Miocene paleobathymetry of the Vienna Basin (Austria). *Marine and Petroleum Geology* 132, 105187. https://doi.org/10.1016/j.marpetgeo.2021.105187

Kranner M., Harzhauser M., Mandic O., Strauss P., Siedl W. & Piller W.E. 2021b: Trends in temperature, salinity and productivity in the Vienna Basin (Austria) during the early and middle Miocene, based on foraminiferal ecology. *Palaeogeography, Palaeoclimatology, Palaeoecology* 581, 110640. https://doi.org/10.1016/j.palaeo.2021.110640

Langer M.R. 1988: Recent epiphytic Foraminifera from Vulcano (Mediterranean Sea). In: Benthos '86. 3rd Int. Syrup. Benthic Foraminifera. (Geneva, Switzerland, September 22–28, 1988.) *Revue de Paleobiologie* 2, 827–832.

Langer M.R. 1993: Epiphytic foraminifera. *Marine Micropaleontology* 20, 235–265.

Laskarev V. 1924: Sur les équivalents du Sarmatien supérieur en Serbie. In: Vujević P. (Ed.): Recueil de travaux offert à M. Jovan Cvijic par ses Amis et Collaborateurs. *Drzhavna Shtamparija*, Beograd, 73–85.

Łuczkowska E. 1964: The micropaleontological stratigraphy of the Miocene in the region of Tarnobrzeg–Chmielnik. *Prace Geologiczne Komisji Nauk Geologicznych PAN, Oddzial w Krakowie* 20, 1–52.

Łuczkowska E. 1971: A new zone with *Praeorbulina indigena* (Foraminiferida, Globigerinidae) in the Upper Badenian (Tortonian s.s.) of Central Paratethys. *Rocznik Polskiego Towarzystwa Geologicznego* 3, 445–448.

Łuczkowska E. 1972: Miliolidae (Foraminiferida) from Miocene of Poland Part I. Revision of the classification, *Acta Palaeontologica Polonica* 17, 342–377.

Łuczkowska E. 1974: Miliolidae (Foraminiferida) from the Miocene of Poland Part II. Biostratigraphy, palaeoecology, and systematics. *Acta Palaeontologica Polonica* 19, 3–176.

Martini E. 1971: Standard Tertiary and Quaternary calcareous nannoplankton zonation. In: Proceedings of the 2nd Planktonic Conference, Roma, 739–785.

Masuiradze L.S. 1971: Foraminifery sarmata Zapadnoi Gruzii [The Foraminifera of Western Georgia Sarmatian]. *Metsniereba,* Tbilisi, 1–120 (in Russian).

Mazzini I., Hudáčková N., Joniak P., Kováčová M., Mike, T., Mulch A., Rojay B., Lucifora S., Esu D. & Soulié-Märsche I. 2013: Palaeoenvironmental and chronological constraints on the Tuğlu Formation (Çankiri Basin, Central Anatolia, Turkey). *Turkish Journal Of Earth Sciences* 22, 1–26.

McCrea J.M. 1950: On the Isotopic Chemistry of Carbonates and Paleotemperature Scale. *Journal of Chemical Physics* 18, 849–857. https://doi.org/10.1063/1.1747785

Meszároš Š. 1986: Anomálie schránok mäkkýšov z vrchnobádenských sedimentov lokalít okolia Malých Karpát. *Západné Karpaty, séria Paleontológia* 11, 57–76 (in Slovak).

Microsoft Corporation 2018: *Microsoft Excel*, Available at: https://office.microsoft.com/excel

Murray J.W. 1991: Ecology and Paleoecology of Benthic Foraminifera. *John Wiley and Sons*, New York, 1–320.

Murray J.W. 2006: Ecology and Applications of Benthic Foraminifera. *Cambridge University Press*, New York, 1–426.

Naidu P.D. & Niitsuma N. 2004: Atypical $d^{13}C$ signature in *Globigerina bulloides* at the ODP site 723A (Arabian Sea): implications of environmental changes caused by upwelling. *Marine Micropaleontology* 53, 1–10.

Neubauer T.A., Harzhauser M., Kroh A., Georgopoulou E. & Mandic O. 2015: A gastropod-based biogeographic scheme for the European Neogene freshwater systems. *Earth-Science Reviews* 143, 98–116.

Nevesskaja L.A., Goncharova I.A., Paramonova N.P., Popov S.B., Babak E.B., Bagdasarjan K.G. & Voronina A.A. 1993: Opredelitelj miocenovj ih dvustvorchatjihmolljuskov Jugo-Zapadnoi Evrazii. *Nauka*, Moskow, 1–412.

Palcu D.V., Tulbure M., Bartol M., Kouwenhoven T.J. & Krijgsman W. 2015: The Badenian–Sarmatian Extinction Event in the Carpathian foredeep basin of Romania: Paleogeographic changes in the Paratethys domain. *Global and Planetary Change* 133, 346–358.

Parker J.H. 2017: Ultrastructure of the test wall in modern porcelaneous foraminifera: Implications for the classification of the miliolida. *Journal of Foraminiferal Research* 47, 136–174.

Pawlowski J., Holzmann M. & Tyszka J. 2013: New supraordinal classification of Foraminifera: Molecules meet morphology. *Marine Micropaleontology* 100, 1–10.

Peryt D., Gedl P., Jurek K., Więcław D., Worobiec E., Worobiec G. & Peryt T.M. 2024: Environmental perturbations around the Badenian/Sarmatian (Middle Miocene) boundary in the Central Paratethys: Micropalaeontological and organic geochemical records. *Palaeogeography, Palaeoclimatology, Palaeoecology* 667, 112221. https://doi.org/10.1016/j.palaeo.2024.112221

Piller W.E. & Harzhauser M. 2005: The myth of the brackish Sarmatian Sea. *Terra Nova* 17, 450–455. https://doi.org/10.1111/j.1365-3121.2005.00632.x

Piller W.E., Harzhauser M. & Mandic O. 2007: Miocene Central Paratethys stratigraphy – Current status and future directions. *Stratigraphy* 4, 151–168. https://doi.org/10.29041/strat.04.2.09

Popov S.V., Rögl F., Rozanov A.Y., Steininger F.F., Shcherba I.G. & Kováč M. (Eds.) 2004: Lithological–Paleogeographic maps of Paratethys. 10 Maps Late Eocene to Pliocene. *Courier Forschungsinstitut Senckenberg* 250, 1–46.

R Development Core Team 2016: R: A Language and Environment for Statistical Computing. *R Foundation for Statistical Computing*, Vienna.

Raffi I., Wade B., Pälike H., Beu A. Cooper R., Crundwell M., Krijgsman W., Moore T., Raine I., Sardella R. & Vernyhorova Y. 2020: The Neogene Period. *Geologic Time Scale 2020.* https://doi.org/10.1016/B978-0-12-824360-2.00029-2

Rögl F. 1998: Palaeogeographic Considerations for Mediterranean and Paratethys Seaways (Oligocene to Miocene). *Annalen des Naturhistorischen Museums in Wien* 99A, 279–310.

Rögl F. 1999: Mediterranean and Paratethys. Facts and hypotheses of an Oligocene to Miocene paleogeography (short overview). *Geologica Carpathica* 50, 339–349.

Rögl F. & Steininger F.F. 1983: Vom Zerfall der Tethys zu Mediterran und Paratethys. Die neogene Paläogeographie und Palinspastik des zirkum-mediterranen Raumes. *Annalen des Naturhistorischen Museums in Wien* 85A, 135–163.

Rögl F., Steininger F.F. & Müller C. 1978: Middle Miocene salinity crisis and paleogeography of the Paratethys (Middle and Eastern Europe). *Initial reports of the Deep Sea Drilling Project* 42, 985–990.

Rohalová M. & Hash J. 2000: Rohožník-Konopiská, ťažobný priestkum. *Záverečná správa, Hirocem*.

Ruman A., Rybár S., Hudáčková N., Šujan M. & Halásová, E. 2017: Depositional environment changes at the Early – Late Serravallian boundary dated by the Central Paratethys bioevents. *Facies* 63, 1–13. https://doi.org/10.1007/s10347-016-0490-8

Šarinová K., Rybár S., Halásová E., Hudáčková N., Jamrich M., Kováčová M. & Šujan M. 2018: Integrated biostratigraphical, sedimentological and provenance analyses with implications lithostratigraphic ranking: the Miocene Komjatice Depression of the Danube Basin. *Geologica Carpathica* 69, 382–409. https://doi.org/10.1515/geoca-2018-0023

Sen Gupta B.K. 2003: Modern foraminifera. *Kluwer Academic Publishers*, New York.

Seneš J. 1961a: Paleogeography of the central part of the Paratethys Sea. In: Murgeanu G., Patrulius D., Tocorjescu M., Contescu L., Jipa D., Mihailescu N., Bombita G., Panin N., Butac A., Filipescu M.G., Alexandrescu Gr., Mutihac V., Sandulescu M., Sandulescu J., Bratu E. & Iliescu G. (Eds.): Ghidul excursiilor B carpatii orientali. Asociatia Carpato–Balcanica, Congresulal V-lea, 4.–9. Septembrie, Bucuresti, 51–52 (in Russian).

Seneš J. 1961b: Paläogeographie des westkarpatischen raumes in beziehung zur übrigen Paratethys im Miozän. *Geologické Práce, Zošit* 60, 159–195.

Shackelton N.J. 1974: Attainment of isotopic equilibrium between ocean water and the benthonic foraminifera genus Uvigerina: isotopic changes in the ocean during the last glacial. *Les Méthodes quantitatives d'étude des variations du climat au cours du pléistocène* 219*,* 203–209.

Shackleton N.J. 1987: The carbon isotope record of the Cenozoic: history of organic carbon burial and of oxygen in the ocean and atmosphere. In: Brooks J. & Fleet A.J. (eds.): Marine petroleum source rocks. *Special Publications – Geological Society London* 26, 423–434.

Spero H.J. & Lea D.W. 1993: Intraspecific stable isotope variability in the planktic foraminifera *Globigerinoides sacculifer*: Results from laboratory experiments. *Marine Micropaleontology* 22, 221–234.

Steineck P.L. & Bergstein J. 1979: Foraminifera from Hommocks salt-marsh, Larchmont Harbor, New York. *Journal of Foraminiferal Research* 9, 147–158.

Steininger F.F. & Rögl R. 1984: Paleogeography and palinspastic reconstructions of the Neogene of the Mediterranean and Paratethys. In: Dixon J.E. & Robertson A.H.F. (Eds.): The Geological Evolution of the Eastern Mediterranean. *The Geological Society London*, 659–668.

Steininger F., Rögl F. & Martini E. 1976: Current Oligocene/Miocene biostratigraphic concept of the Central Paratethys (Middle Europe). *Newsletters on Stratigraphy* 4, 174–202.

Švagrovský J. 1971: Das Sarmat der Tschechoslowakei und seine Molluskenfauna. *Acta Geologica et Geografica Universitatis Comenianae Geologica* 20, 1–473.

Švagrovský J. 1981: Lithofazielle Entwicklung und Molluskenfauna des oberen Badeniens (Miozän M4d) in dem Gebiet Bratislava – Devínska Nová Ves. *Západné Karpaty, séria Paleontológia* 7, 5–204.

Tóth E., Görög A., Lecuyer V., Moissette P., Balter B. & Monostori M. 2010: Paleoenvironment reconstruction of the Sarmatian (Middle Miocene) centra Paratethys based on paleontological and geochemical analyses of foraminifera, ostracods, gastropods and rodents. *Geological Magazine* 147, 299–314. https://doi.org/10.1017/S0016756809990203

Tribovillard N., Algeo T.J., Lyons T. & Riboulleau A. 2006: Trace metals as paleoredox and paleoproductivity proxies: an update. *Chemical Geology* 232, 12–32. https://doi.org/10.1016/j.chemgeo.2006.02.012

Urey H.C. 1947: The thermodynamic properties of isotopic substances. *Journal of the Chemical Society* (Resumed), 562–581.

Vass D. 2002: Litostratigrafia Západných Karpát: neogén a budínsky paleogén [Litostratigraphy of Western Carpathians: Neogene and Buda Paleogene)]. *Štátny geologický ústav D. Štúra*, Bratislava, 1–202 (in Slovak with English summary).

Wade B.S., Pearson P.N., Berggren W.A. & Pälike H. 2011: Review and revision of Cenozoic tropical planktonic foraminiferal biostratigraphy and calibration to the geomagnetic polarity and astronomical time scale. *Earth-Science Reviews* 104, 111–142. https://doi.org/10.1016/j.earscirev.2010.09.003

Weldeab S., Lea D.W., Schneider R.R. & Andersen N. 2007: 155,000 years of West African monsoon and ocean thermal evolution, *Science* 316, 1303–1307. https://doi.org/10.1126/science.1140461

Zahradníková B., Hudáčková N., Halásová E., Rybár S. & Kováč M. 2013: New findings from research of Sarmatian sediments from Ivanka-l well (Danube Basin, Slovakia). *Acta Rerum Naturalium Musei Nationalis Slovaci* 59, 25–32.

Zlinská A., Hudáčková N. & Koubová I. 2010: Lower Sarmatian foraminifera from marginal marine environments in the Malacky vicinity (Vienna Basin). *Geologické výzkumy na Moravě a ve Slezsku* 17, 104–106.

Electronic supplementary material is available online at http://geologicacarpathica.com/data/files/supplements/GC-75-4-Babejova-Kmecova_Supplement.pdf